Optimizing blockchain-enabled sustainable supply chains

Jingwen Wu, Yuting Yan, Shuaian Wang, Lu Zhen

This work was supported by the National Natural Science Foundation of China (Grant numbers 72025103, 72394360, 72394362, 72361137001, 72071173, 72371221), the Project of Science and Technology Commission of Shanghai Municipality China (grant number 23JC1402200), and HKSAR RGC TRS T32-707/22-N]. (Corresponding authors: Lu Zhen).

Jingwen Wu, Yuting Yan, and Lu Zhen are with the School of Management, Shanghai University, Shanghai 200444, China (e-mails: jingwen_wu@shu.edu.cn, yanzi@shu.edu.cn, lzhen@shu.edu.cn). Shuaian Wang is with Faculty of Business, The Hong Kong Polytechnic University, Hung Hom, Hong Kong, China (e-mail: hans.wang@polyu.edu.hk).

Abstract: The increasing pressure on global supply chains to reduce carbon emissions has driven the need for sustainable supply chain network design (SSCND). This paper proposes an innovative framework for SSCND that optimizes facility location and scale decisions under uncertainty using blockchain technology. By incorporating cap-and-trade regulations and carbon trading into a mixed-integer linear programming model, the study addresses both the economic and environmental objectives of supply chains. A two-stage stochastic programming approach is employed to optimize the SSCND. The first stage focuses on facility location decisions and the second stage on production adjustment, transportation, and carbon trading under demand uncertainty. The carbon trading decisions are integrated into the model by assigning a monetary value to carbon dioxide emissions and allowing for dynamic adjustments to real-time environmental impacts. A primal decomposition algorithm is introduced to address the computational challenges involved in solving the two-stage stochastic programming model. Numerical experiments based on data derived from SAIC Motor Corporation's supply chain demonstrate the effectiveness of the model and algorithm. This study provides an efficient approach for integrating environmental sustainability into supply chain management, offering valuable insights for industries aiming to achieve carbon neutrality.

Keywords: Sustainable supply chain network design; blockchain; smart contract; cap-and-trade regulation; primal decomposition algorithm.

Managerial relevance statement: This study provides valuable insights for manufacturing managers and policymakers seeking to optimize sustainable supply chains. By integrating blockchain technology and carbon trading mechanisms, the proposed model enables more efficient facility location decisions, production adjustments, and transportation strategies under demand uncertainty. Managers in manufacturing companies can use this framework to enhance the transparency and traceability of carbon emissions while making cost-effective, data-driven decisions that align with sustainability goals. The research highlights that accurately forecasting demand fluctuations and strategically allocating carbon quotas—particularly by allocating sufficient quotas to logistics centers—can significantly reduce carbon credit purchasing costs. Policymakers can leverage these insights to adjust carbon quota policies

and promote the adoption of green transportation and low-carbon technologies. An unexpected finding is that, under the regulatory pressure of cap-and-trade policies, blindly increasing production to meet uncertain demand results in higher costs. This suggests that manufacturing companies should carefully align production capacity with actual demand, avoiding overproduction that may result in additional costs under the carbon trading system. They should also assess demand fluctuations thoroughly and avoid excessive reliance on unstable market demands.

1. Introduction

Supply chain operations significantly contribute to global CO_2 emissions. At the supplier stage, raw material transformation into semi-finished goods generates substantial hydrocarbons and acidic compounds, including sulfur oxides. For instance, steel manufacturing alone accounts for approximately 7% of global CO_2 emissions. The logistics phase further exacerbates emissions, varying with transportation methods, fuel types, and distances [1]. For example, Perez-Martinez et al. [2] report emission factors of 2.3 km/L for 40-ton class 8 trucks and 8.2 km/L for diesel vans, translating to about 3,800 g CO_2 per kg of fuel. These emissions collectively drive global warming, intensifying climate-related disasters. To mitigate these impacts, governments worldwide have adopted various carbon policies and mechanisms [3]. Among these, cap-and-trade regulations are acknowledged as one of the most successful market-based approaches for controlling corporate emissions. Under cap-and-trade schemes, firms exceeding quotas must purchase credits, while those with surplus credits can sell them for profit, fostering accountability and incentivizing sustainability [4].

Cap-and-trade regulations make it crucial for businesses to achieve specific sustainability objectives [5]. In response to pressures to prioritize environmental sustainability, businesses increasingly incorporate blockchain technology into their supply chain networks. Blockchain offers transparency, immutability, and decentralization [6],[7],[8], enabling real-time sharing of carbon emission data, streamlining carbon trading, and enhancing the credibility of transactions. By ensuring transparency, enhancing data security, and providing immutable transaction records, blockchain can optimize carbon emission tracking and simplify verifying sustainability practices across the supply chain. This is particularly crucial in carbon trading and regulatory compliance, where accountability and trust are essential. Therefore, by integrating blockchain with supply chain management (SCM), businesses not only enhance the efficiency of their operations but also contribute to their sustainability goals [9],[10].

However, integrating blockchain into supply chain management presents several key challenges, such as ensuring data integrity, creating efficient and scalable smart contract mechanisms, and ensuring the traceability of transactions in dynamic environments. Motivated by SAIC Motor Corporation's need for sustainable, low-carbon strategies, this study proposes a blockchain-based decision framework inspired

by Manupati et al. [9]. Our framework integrates smart contracts with real-time operational decisions, enabling automatic execution of carbon trading and production adjustments under predefined blockchain protocols. Unlike Manupati et al. [9], who focus solely on production allocation under carbon tax policies, our approach incorporates demand uncertainty and carbon trading, expanding the scope of decision-making and enhancing the adaptability of supply chains to real-world complexities. This dynamic interaction between blockchain and SCM ensures compliance, flexibility, and scalability, addressing the challenges of modern supply chain operations.

Specifically, our model addresses demand uncertainty in supply chains through a two-stage stochastic programming approach. The first stage involves making strategic facility location decisions. In contrast, the second stage focuses on operational adjustments, such as modifying production quantities, altering transportation plans, and making carbon trading decisions in response to demand fluctuations. The academic literature shows that the two-stage framework, where the first stage involves strategic planning and the second stage focuses on tactical adjustments to real-world uncertainties, is widely used and effective in addressing uncertainty and multi-level decision-making problems across various domains [11],[12],[13]. Furthermore, to address the increased complexity introduced by integer decision variables in the two-stage stochastic model, we propose a primal decomposition algorithm. Similar to Benders decomposition, our algorithm differs in that it transmits primal columns from the second-stage subproblem to the first-stage master problem, whereas Benders uses dual-based cuts (rows). Our algorithm is particularly effective when the second-stage subproblem involves integer variables, a scenario where traditional Benders decomposition is not applicable.

To summarize, the contribution of this work is twofold. From a practical perspective, this study responds to the need for sustainable supply chains under cap-and-trade regulations and the challenges posed by demand uncertainty in manufacturing enterprises. By integrating blockchain technology, the model addresses key issues such as inefficiency, lack of trust, and insufficient data security in traditional supply chains, ensuring transparency and secure data sharing. Additionally, incorporating carbon trading mechanisms offers a cost-effective approach to achieving both environmental and economic goals, enabling manufacturers to optimize facility location, production, and transportation strategies under uncertainty. From an academic perspective, while numerous studies have explored blockchain technology in supply chain management [14],[15],[16],[17],[18], most have focused on the conceptual and functional characteristics of blockchain, with limited attention given to its integration within mixed-integer mathematical models for supply chain optimization. To our knowledge, this study is the first to combine blockchain technology with carbon trading mechanisms in the context of sustainable supply chain network design under demand uncertainty. By employing a mathematical modeling approach, this

research contributes to supply chain optimization and environmental sustainability, enriching and extending the current literature.

This paper is structured as follows. Section 2 reviews the related literature. Section 3 provides a comprehensive explanation of the problem. Section 4 presents a mixed-integer linear programming (MILP) model for the two-stage decision-making process. Section 5 introduces the algorithm for solving the model. Section 6 presents the numerical experiments conducted to validate the model and algorithm. The final section concludes the paper with a summary of the study's key insights.

2. Related works

The main contribution of this study lies in applying blockchain technology to address the challenge of sustainable supply chain network designs (SSCND). We provide a framework for making decisions regarding facility location and scaling under uncertainty utilizing blockchain to enhance the management of sustainable supply chains. The literature on this topic focuses on two key areas: SSCND under uncertainty and the application of blockchain and smart contract technologies in SCM.

2.1 SSCND under uncertainty

Supply chain network design (SCND), or strategic supply chain planning, involves critical long-term decisions shaping a business's success [19]. It focuses on defining supply chains' infrastructure and physical layout, including facility locations, capacities, production processes, technologies, regional distribution, and supplier selection, all requiring significant investment. [20]. Recently, sustainable supply chains have garnered increasing attention due to pressure from various stakeholders, such as consumers, management, government regulators, and community activists, and global competition [21],[22]. This emphasis on sustainability has driven research on SSCND, in which initial investments in introducing facilities across various locations and capacity allocation are crucial as they significantly influence environmental outcomes during the operational phase [23]. However, SSCND is further complicated by market uncertainty and limited resources in real-world scenarios [24]. Addressing these uncertainties has thus become a central focus of academic researchers and industry practitioners. To successfully do so, a thorough grasp of the challenges and opportunities in this domain is crucial, as emphasized by key studies on SSCND [20],[25],[26].

The primary approach to modeling sustainable supply chain networks under uncertainty is to use carbon emissions as an environmental indicator while addressing various uncertainties specific to the problem at hand. For instance, Pishvaee et al. [27] introduce a bi-objective fuzzy mathematical programming model to design green logistics networks under uncertain conditions, employing the CO_2 equivalent index to evaluate environmental impacts. Zhen et al. [28] present a comprehensive

methodology for designing a green and sustainable closed-loop supply chain network in the face of uncertain demand. They propose a bi-objective optimization model that minimizes CO_2 emissions and total operational costs, incorporating environmental standards and the factors influencing facility capacity in the decision-making process. Kaur et al. [29] further enhance the understanding of sustainable supply chain modeling by proposing an elastic, sustainable framework that integrates production and procurement through fuzzy theory. This approach addresses market demand and machine capacity uncertainties while accounting for carbon emissions. Similarly, Hasani et al. [30] contribute a robust multi-objective optimization model for configuring a green global supply chain network amidst disruptions and uncertainties. Their model simultaneously optimizes three objectives: maximizing expected profit, minimizing facility centralization to mitigate disruptions, and reducing CO_2 emissions related to material shipments within the sustainable network. Furthermore, Kumar et al. [31] propose an MILP model for designing uncertain supply chain networks, considering both carbon emissions and social factors and utilizing chance-constrained programming to address uncertainty.

Based on the aforementioned research trends, this study evaluates a sustainable supply chain using two key environmental indicators: the fixed CO_2 emissions of facilities at various emission control levels and the CO_2 emissions due to transportation. Additionally, it considers demand uncertainty, an important factor in realistic scenarios, to further extend research on the design of sustainable supply chain networks.

2.2 Modeling supply chains using blockchain and smart contracts

Blockchain technology provides a shared, distributed database with unique features such as cryptographic security, immutability, traceability, and intelligent execution [32],[33]. These characteristics help address the complexity and critical challenges involved in SCM, particularly in ensuring transparency, reliability, and efficiency [34],[35]. Blockchain technology is being increasingly adopted in low-carbon supply chains, enabling consumers to oversee the processes of producing low-carbon products. This enhanced transparency improves brands' reputations and presents new market opportunities [36]. With growing environmental awareness among the public, an increasing number of consumers are willing to pay a premium for sustainable products [37], and sustainability has become a key factor in corporate performance [38]. In response, major corporations such as Walmart, Alibaba [39], De Beers, UPS, and FedEx have adopted blockchain to enhance transparency and monitor their carbon footprints, promoting sustainable practices.

Research consistently shows that sustainable supply chains can greatly benefit from the adoption of blockchain technology [40]. In the context of fashion supply chains, Choi et al. [41] emphasize the

advantages of blockchain, particularly in emerging markets such as China and India, where transparency and traceability are increasingly important. Building on their study, Guo et al. [42] find that blockchain facilitates environmental transparency and increases consumers' willingness to spend on sustainable fashion products. In addition to its impact on the fashion industry, blockchain has proven effective in other sectors. For instance, El Hathat et al. [43] demonstrate its utility in tracing greenhouse gas emissions in the palm oil supply chain, ultimately enhancing sustainability and competitiveness. Similarly, Xu et al. [44] illustrate how blockchain can optimize remanufacturing operations, particularly for high-emission industries, by integrating manufacturers, third-party companies, and online platforms into a more efficient system. Further advancing this understanding, Yousefi et al. [45] develop a systems analysis approach to assess the broader impact of blockchain on sustainable supply chains. Their findings suggest that the appropriate adoption of blockchain can significantly improve environmental sustainability and increase the traceability of products. Blockchain's potential also extends to agricultural supply chains, in which it helps address sustainability challenges [46] and advances the adoption of circular economy principles [47].

Smart contracts, a crucial application of blockchain technology [48], are computer programs that automatically execute, control or document the terms of a contract. In a system that uses smart contracts, participants create their contracts by specifying the code and implementing it on the blockchain. When predefined conditions are met, the contract's terms are automatically executed. In SCM, this technology can significantly enhance efficiency, transparency, and traceability while reducing disputes and the risk of fraud. The effective implementation of blockchain technology across different industries requires the definition and execution of smart contracts using various mathematical models and algorithms [49]. For instance, Li et al. [50] design an innovative and practical framework for emissions trading in the road transport sector utilizing cutting-edge blockchain technology. In their system, all transactions related to emission permits are efficiently managed and recorded through smart contracts on a decentralized blockchain. This approach results in a significant reduction in management costs. Similarly, Agrawal et al. [51] propose a traceability framework based on blockchain technology, incorporating customized smart contracts and transaction protocols. Using the example of an organic cotton supply chain, they demonstrate how a blockchain-based, traceable, multi-layer textile and apparel supply chain system can enhance sustainability and ensure transparency for all stakeholders. Expanding on this, Sadawi et al. [52] introduce a multi-layered blockchain framework within the Blockchain of Things (BoT), incorporating smart contracts to design a refined carbon emissions trading system characterized by transparency and automated trading and control processes. Building further on the integration of blockchain in supply chains, Ismail et al. [53] combine blockchain technology with emerging

technologies such as artificial intelligence (AI) and the Internet of Things (IoT) to propose a blockchain-based fish supply chain framework. By utilizing the core functions of blockchain and smart contracts deployed on the Ethereum platform, their approach ensures the integrity and security of fish supply chain data.

In conclusion, the rise of blockchain technology has established smart contracts as a leading technology, enhancing the customization of traditional transactions in carbon trading markets. This study uses smart contracts to integrate carbon trading decisions into SCND problems and designs smart contract rules to implement carbon trading decisions. The proposed approach balances economic and environmental considerations in the supply chain and thus enriches the literature in this field.

2.3 Summary of related works

A review of the literature reveals that although significant advancements have been made in the domain of SSCND, several critical research gaps remain to be addressed.

First, previous studies, such as those by Zhen et al. [28] and Hasani et al. [48], primarily focus on minimizing CO_2 emissions and optimizing costs under uncertainty but do not effectively integrate market-based carbon trading mechanisms into the design of supply chain networks. Their models optimize supply chain performance based on emission reductions, but they overlook the dynamic role that carbon trading plays in facility location and scaling decisions. This study differs by incorporating carbon trading as a pivotal factor in the decision-making process, accounting for environmental goals and market-driven carbon management strategies.

Second, although blockchain and smart contracts are heralded for their potential to improve supply chains' transparency and operational efficiency, challenges to their widespread implementation still exist [54]. Most research focuses on blockchain's role in operational processes such as transaction tracking and verification. Few studies explore its application to decision-making in SSCND, particularly concerning facility locations and carbon trading. This study bridges this gap by integrating blockchain technology and a two-stage stochastic programming model into SSCND to facilitate facility location, scaling, and carbon trading decisions under uncertainty. This approach represents a novel application of blockchain to SSCND beyond its traditional use to achieve operational improvements.

Finally, although uncertainties in demand, costs, and environmental factors are widely acknowledged as challenging to SSCND, existing models addressing these uncertainties using fuzzy or stochastic approaches fall short when applied to large-scale supply chains. In this study, the proposed primal decomposition algorithm improves the computational efficiency of the stochastic model and provides a robust solution to large-scale SCND problems. Unlike those used in earlier models, this algorithm

effectively handles the complexities of integrating blockchain, smart contracts, and carbon trading into a sustainable supply chain, making it a significant methodological contribution to the study.

3. Problem description

This paper focuses on using blockchain and smart contract technologies to optimize decision-making regarding facility locations and scale in a sustainable supply chain network. In this section, we introduce the proposed blockchain decision-making framework and describe the first and second stages of the decision-making process outlined in the framework.

3.1 Decision-making process framework under blockchain

To address the challenge of uncertain demand, we develop a two-stage stochastic programming model to optimize sustainable supply chain networks for manufacturing enterprises facing increasing pressure due to carbon cap-and-trade regulations. Our objective is to minimize overall carbon emissions and supply chain costs. By integrating blockchain technology, our model enhances operational efficiency, transparency, and trust in the supply chain network while reducing human intervention and improving decision-making accuracy. The decision-making process consists of two stages: the first stage focuses on strategic planning to establish a baseline schedule that meets specific demands, whereas the second stage concentrates on operational adjustments based on demand fluctuations in realistic scenarios.

The decision-making process and the key decision-making characteristics of the two stages under the framework of the blockchain mechanism are shown in Figure 1. The first step involves deploying smart contracts throughout a sustainable supply chain, ensuring their presence across nodes. By utilizing distributed ledger technology in the form of smart contracts, we can effectively capture and transmit real-time transaction data and carbon emission information from every node within the supply chain. This valuable data is then securely added to the blockchain for seamless stakeholder sharing. Subsequently, leveraging this blockchain-based information alongside smart contracts enables us to provide decision support through a two-stage stochastic programming model and primal decomposition algorithm integrated into our decision support system. Smart contracts play a key role by establishing predefined rules based on carbon threshold conditions. Once activated, they enable continuous monitoring of carbon emissions at each node in real-time. In instances where carbon emissions exceed allocated limits (in Figure 1， e_s^F and e_l^R represent the carbon quotas of the producers and logistics centers, respectively), an alert is triggered by the smart contract, prompting necessary adjustments to be made within the current plan or facilitating carbon trading activities maintain emissions levels within acceptable thresholds.

The details of the decision-making framework, such as the optimal location with the consideration of facility scales and the carbon trading decision, are detailed in Sections 3.2 and 3.3, respectively.

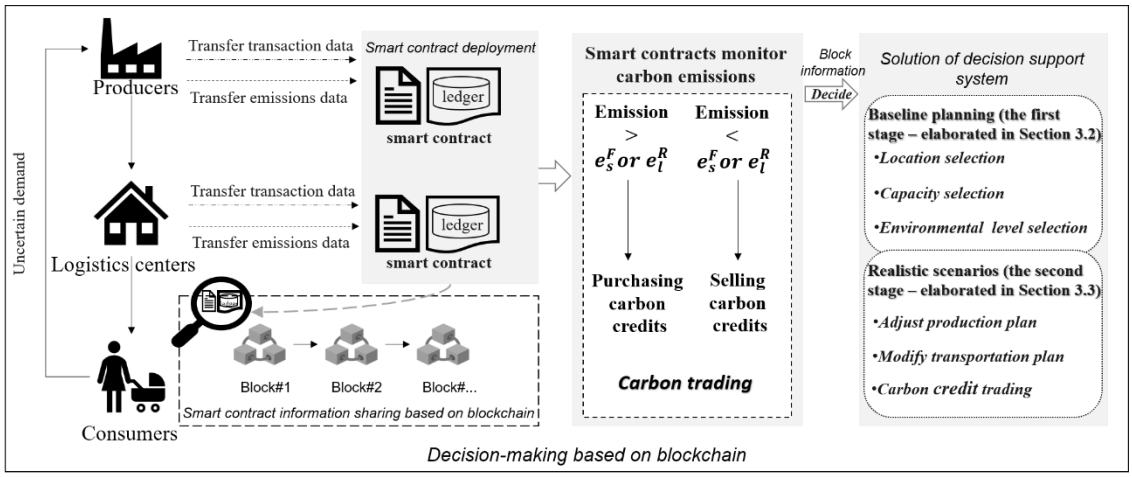

Figure 1: Supply chain network optimization framework based on blockchain

3.2 The first stage of decision-making under the blockchain

The primary objective of the first stage of the decision-making process is to determine the optimal locations and scales of producers and logistics centers given specific capacity and emission control levels while minimizing the total cost of meeting customer demand. This stage establishes an initial baseline plan at the strategic level. Specifically, we determine a set of producers and logistics centers with constraints on capacity and emission control levels. Emission control levels are quantified by CO_2 emissions, such that lower emissions correspond to higher control levels. Following the methodology of Zhen et al. [28], we categorize the levels of capacity and emission control into discrete values, "1," "2," and "3," with higher numbers representing higher levels of capacity and environmental performance, respectively, but also higher costs. The supply chain must select producers (denoted by α_{scb}) and logistics centers (denoted by β_{lcb}) with suitable capacity levels (indexed by b) and emission control levels (indexed by c) from the candidate sets of producer sites S and logistics center sites L to satisfy customer demand (denoted by d_k). The total production and processing volume at each node (denoted by μ_{sl} and θ_{lk}) must not exceed the node's capacity level. The products produced by producers are first transported to various logistics centers for processing and then delivered to customers. Product flow between producers and logistics centers must be balanced during transportation. Blockchain's distributed ledger technology plays a crucial role in this stage by recording the initialization of multi-layer supply chain data variables and enabling information sharing among stakeholders. The ledger collects and records transaction and emissions data, which are passed on as goods move through the supply chain. Our model uses this data to preprocess and calculate the quantities of products processed and transported at each node and the initial optimal cost, thereby

establishing an initial baseline plan for the optimal locations and scales of facilities.

3.3 The second stage of decision-making under the blockchain framework

Building on the selection of locations and scales from the first stage, the second stage addresses the challenge of uncertain demand (denoted by $\tilde{d}_{\omega k}$) by adjusting the production and transportation plans and ensuring that the carbon emission of each node (for example, denoted by q_{cs}^{F} and q_{cl}^{R} for producers and logistics centers, respectively, with emission control level c; this value is the sum of the node's fixed CO_2 emissions) does not exceed the specified carbon quota (denoted by e_s^F and e_l^R) of the node. Through this process, we aim to optimize overall supply chain costs and effectively reduce carbon emissions, achieving an optimal operational decision plan.

Blockchain's smart contract technology plays a crucial role in this stage. Smart contracts can record and track carbon emissions and goods transfer data in real-time, treating carbon emissions as tradable carbon credits (one carbon credit equals the right to emit 1000 kg of CO_2 equivalent) and sharing this data on a distributed ledger. Using the blockchain-enabled system, each supply chain node initializes a smart contract, which triggers an alert when emissions exceed a threshold, indicating that they surpass the carbon quota. This real-time monitoring and automatic alert system significantly enhances the transparency and responsiveness of SCM.

Specifically, in the second stage of the decision-making process, our model simulates the threshold constraints encoded in smart contracts by setting carbon quota limits (i.e., e_s^F and e_l^R) for producers and logistics centers. After the smart contract is activated, it monitors the carbon emissions of each node in the supply chain in real-time and transmits this information on the blockchain. This enables our decision support system to readjust decisions based on the actual needs of each node in a real-world scenario. For example, demand uncertainty may cause the actual processing and transportation of goods by supply chain nodes (denoted by $\tilde{\theta}_{\omega lk}$ and $\tilde{\mu}_{\omega sl}$) to deviate from the baseline plan (i.e., μ_{sl} and θ_{lk}), resulting in the total CO_2 emissions at each node exceeding or falling below its specified carbon quota. Enterprises can offset the excess or shortfall in carbon emissions by purchasing or selling carbon credits (denoted by $\tilde{\zeta}_{\omega s}^{+}$ or $\tilde{\zeta}_{\omega s}^{-}$ for producers and $\tilde{\eta}_{\omega l}^{+}$ or $\tilde{\eta}_{\omega l}^{-}$ for logistics sites, respectively) in the carbon trading market, keeping emissions within set thresholds and minimizing penalties. Thus, in the second stage, we innovatively incorporate carbon trading into the total supply chain cost, assigning a monetary value to carbon emissions and integrating environmental impact into the economic analysis of the supply chain. Note that in this process, some customer demand may be abandoned due to the consideration of emission reduction, and the unmet demand may result in certain losses to the supply chain. Therefore, we penalize logistics centers for unmet customer demand to reflect the potential losses

to the entire supply chain.

By calculating the total cost of the current supply chain and incorporating it into the two-stage decision-making process, our decision support system addresses different demand scenarios to ensure the best overall operation in each scenario. The iterative data sharing and optimization process is executed until the optimal solution is found. Therefore, in the second stage, in which demand uncertainty is addressed, our framework minimizes the expected operating and carbon trading costs in each scenario to determine the volume of goods produced and transported and the carbon credits purchased and sold by each supply chain node. This process results in the actual plan for scheduling decisions (at the operational level) across various demand scenarios.

4. Two-stage model

Our two-stage stochastic programming model addresses the SSCND problem under demand uncertainty. The model accounts for each facility's capacity and carbon emission levels, uncertain customer demand, production or processing costs, transportation costs, delivery and holding costs, and carbon credit transaction costs. The overall cost consists of two components: fixed costs and estimated operating expenses. As scenario-based programming is typically adopted to address parameter uncertainties, we represent uncertainties in our model parameters through a set of scenarios. Our objective is to reduce the total cost across the various scenarios.

4.1 Notations

In this subsection, we list the names of the variables used in the mathematical model. For ease of comprehension, the parameters and decision variables in the mathematical model are represented by Roman and Greek letters, respectively.

Indices and sets

S set of candidate producer sites indexed by s;

L set of candidate logistics center sites indexed by l;

K set of customers indexed by k;

B set of capacity level options of producer sites indexed by b;

C set of emissions control level options of facilities indexed by c;

Ω set of uncertain demand scenarios, indexed by ω.

Parameters

d_k demand of customer k;

$\tilde{d}_{\omega k}$ demand of customer k under scenario ω;

g_{mn}^{c} cost of one truckload products from location m to n, including vehicle transportation cost

and product holding cost (RMB), $m \in S \cup L, n \in L \cup K$;

g_{mn}^{E} CO_2 emissions (in kg) of trucks from location m to n, $m \in S \cup L, n \in L \cup K$;

f_{scb}^{F} fixed cost (RMB) of opening a producer at location s with capacity level b and emissions control level c;

f_{lcb}^{R} fixed cost (RMB) of opening a logistics center at location l with capacity level b and emissions control level c;

m_{sb}^{F} production capacity of producer s with capacity level b;

m_{lb}^{R} processing capacity of logistics facility l with capacity level b;

k_{sb}^{F} unit production cost (RMB) of producer s with capacity level b;

n_{lb}^{R} unit processing cost (RMB) of logistics facility l with capacity level b;

q_{cs}^{F} fixed CO_2 emissions (in kg) with emissions control level c from opening production point s, for example, when c is equal to 1,2,3, respectively, $q_{cs}^{F} = 300,250,200$ kg;

q_{cl}^{R} fixed CO_2 emissions (in kg) with emissions control level c from opening logistics facility l, for example, when c is equal to 1,2,3, respectively, $q_{cl}^{R} = 150,125,100$ kg;

e_{s}^{F} carbon quota (in kg) to producer s;

e_{l}^{R} carbon quota (in kg) to logistics center l;

o_{s}^{F} limited number of carbon credits purchased by producer s;

o_{l}^{R} limited number of carbon credits purchased by logistics center l;

c^{0} market price of carbon credits (RMB);

c^{1} penalty costs (RMB) for not meeting customer needs;

p_{ω} probability of scenario ω with uncertain demand, $\sum_{\omega \in \Omega} p_{\omega} = 1$.

Decision variables

α_{scb} binary, equals one if a producer is built at location s with emissions control level c and capacity level b, $c \in C$, $b \in B$, otherwise, equals zero;

β_{lcb} binary, equals one if a logistics center is built at location l with emissions control level c and capacity level b, $c \in C$, $b \in B$, otherwise, equals zero;

μ_{sl} quantity of product transported from producer s to logistics center l;

θ_{lk} the demand of customer k that is satisfied by logistics center l.

Variables denoted with a tilde ("~") and parameter "ω" correspond to the actual values in scenario ω. For example, the above two variables when denoted with a tilde ("~") and parameter "ω", namely $\tilde{\theta}_{\omega lk}$ and $\tilde{\mu}_{\omega sl}$, refer to the actual values in scenario ω. In addition, decision variables related to carbon trading corresponding to scenario ω are defined as follows.

$\tilde{\zeta}_{\omega s}^{+}$ carbon credits purchased by producer s under scenario ω;

$\tilde{\zeta}_{\omega s}^{-}$ carbon credits sold by producer s under scenario ω;

$\tilde{\eta}_{\omega l}^{+}$ carbon credits purchased by logistics center l under scenario ω;

$\tilde{\eta}_{\omega l}^{-}$ carbon credits sold by logistics center l under scenario ω.

4.2 Mathematical model

Using the definition provided above, M1 is formulated as follows.

4.2.1 Model's objective

The model aims to minimize the total supply chain cost, with the objective function comprising four main components.

(1) The total fixed cost of establishing the producers and logistics centers, FC, is expressed as follows: $FC = \sum_{s\in S}\sum_{c\in C}\sum_{b\in B_s} f_{scb}^{F}\,\alpha_{scb} + \sum_{l\in L}\sum_{c\in C}\sum_{b\in B_l} f_{lcb}^{R}\,\beta_{lcb}$;

(2) The cost of transferring goods from producers to logistics centers, which includes production, transportation, and holding costs, PL, is expressed as follows: $PL = \sum_{s\in S}\sum_{l\in L}\mu_{sl}\left(g_{sl}^{C} + \sum_{c\in C}\sum_{b\in B_s} k_{sb}^{F}\,\alpha_{scb}\right)$;

(3) The cost of delivering goods from logistics centers to customers, including transportation, handling, and holding costs, LC, is expressed as follows: $LC = \sum_{l\in L}\sum_{k\in K}\theta_{lk}\left(g_{lk}^{C} + \sum_{c\in C}\sum_{b\in B_l} n_{lb}^{R}\beta_{lcb}\right)$;

(4) The objective of the subproblem in the second stage, which represents the expected cost of managing uncertain demand across all scenarios, is denoted by $Q(\boldsymbol{\theta}, \omega)$.

Given the above components of the model, the formulation of the model's objective function is expressed as follows.

$[\mathbf{M1}]$ Min $TC = FC + PL + LC + \sum_{\omega\in\Omega} p_{\omega}\,Q(\boldsymbol{\theta}, \omega)$ (1)

4.2.2 The constraints of the first stage

$\sum_{c\in C}\sum_{b\in B_s}\alpha_{scb} \le 1$ $\forall s \in S$ (2)

$\sum_{c\in C}\sum_{b\in B_l}\beta_{lcb} \le 1$ $\forall l \in L$ (3)

$\sum_{l\in L}\theta_{lk} \ge d_k$ $\forall k \in K$ (4)

$\sum_{s\in S}\mu_{sl} = \sum_{k\in K}\theta_{lk}$ $\forall l \in L$ (5)

$\sum_{k\in K}\theta_{lk} \le \sum_{c\in C}\sum_{b\in B_l} m_{lb}^{R}\,\beta_{lcb}$ $\forall l \in L$ (6)

$\sum_{l\in L}\mu_{sl} \le \sum_{c\in C}\sum_{b\in B_s} m_{sb}^{F}\alpha_{scb}$ $\forall s \in S$ (7)

$\theta_{lk}, \mu_{sl} \ge 0$ $\forall s \in S, l \in L, k \in K$ (8)

$\alpha_{s,c,b}, \beta_{l,c,b} \in \{0,1\}$ $\forall s \in S, l \in L, c \in C, b \in B.$ (9)

Constraints (2) and (3) ensure that the producer or logistics center has only one possible capacity level and one possible emission control level. Constraints (4) ensure that the logistics center meets all demands generated by the customer. Constraints (5) ensure the conservation of product flow between the logistics center and the producer. Constraints (6) limit the total volume of products transported to the logistics center to not exceed the volume specified by the capacity level of the center. Constraints (7) limit the capacity of the producer. Constraints (8) and (9) establish the allowable range for the decision variables in the first stage.

4.2.3 The second-stage subproblem's objective

The objective of the subproblem in the second stage consists of three parts: expected operating costs, expected carbon trading costs, and expected penalty costs for unmet demand.

$$\mathcal{Q}(\boldsymbol{\theta}, \omega) = \left(\widetilde{PL} + \widetilde{LC}\right) + c^0\left[\sum_{\omega\in\Omega}\left(\sum_{s\in S}\left(\tilde{\zeta}^+_{\omega s} - \tilde{\zeta}^-_{\omega s}\right) + \sum_{l\in L}\left(\tilde{\eta}^+_{\omega l} - \tilde{\eta}^-_{\omega l}\right)\right)\right] + \sum_{\omega\in\Omega}\sum_{l\in L} c^1\left(\sum_{k\in K}\theta_{lk} - \sum_{k\in K}\tilde{\theta}_{\omega lk}\right)^+ \quad (10)$$

where $\widetilde{PL} = \sum_{\omega\in\Omega}\sum_{s\in S}\sum_{l\in L}\tilde{\mu}_{\omega sl}\left(g^C_{sl} + \sum_{c\in C}\sum_{b\in B_s} k^F_{sb}\,\alpha_{scb}\right)$;

$\widetilde{LC} = \sum_{\omega\in\Omega}\sum_{l\in L}\sum_{k\in K}\tilde{\theta}_{\omega lk}\left(g^C_{lk} + \sum_{c\in C}\sum_{b\in B_l} n^R_{lb}\,\beta_{lcb}\right)$.

The first part (i.e., $\widetilde{PL}$ and $\widetilde{LC}$) represents the actual operating cost in scenario ω, which is similar to the operating cost in the first stage. The second part is the carbon trading cost in scenario ω, represented by $c^0\left[\sum_{\omega\in\Omega}\left(\sum_{s\in S}\left(\tilde{\zeta}^+_{\omega s} - \tilde{\zeta}^-_{\omega s}\right) + \sum_{l\in L}\left(\tilde{\eta}^+_{\omega l} - \tilde{\eta}^-_{\omega l}\right)\right)\right]$. Note that the unit of the decision variable (i.e., $\tilde{\zeta}^+_{\omega s}$, $\tilde{\zeta}^-_{\omega s}$, $\tilde{\eta}^+_{\omega l}$, or $\tilde{\eta}^-_{\omega l}$) is carbon credit, and one carbon credit equals 1,000 kg of CO_2. The last part of the expression $\sum_{\omega\in\Omega}\sum_{l\in L} c^1\left(\sum_{k\in K}\theta_{lk} - \sum_{k\in K}\tilde{\theta}_{\omega lk}\right)^+$ is the penalty cost. It represents the difference between the customer demand handled by a logistics center in the first stage and the customer demand actually handled by the logistics center in scenario ω in the second stage. When the demand handled in the second stage is less than that in the first stage, we penalize the logistics center using a penalty cost c^1.

4.2.4 The constraints of the second stage

$$\sum_{l\in L}\tilde{\theta}_{\omega lk} \le \tilde{d}_{\omega k} \qquad \forall k\in K, \omega\in\Omega \qquad (11)$$

$$\sum_{s\in S}\tilde{\mu}_{\omega sl} = \sum_{k\in K}\tilde{\theta}_{\omega lk} \qquad \forall l\in L, \omega\in\Omega \qquad (12)$$

$$\sum_{k\in K}\tilde{\theta}_{\omega lk} \le \sum_{c\in C}\sum_{b\in B_l} m^R_{lb}\,\beta_{lcb} \qquad \forall l\in L, \omega\in\Omega \qquad (13)$$

$$\sum_{l\in L}\tilde{\mu}_{\omega sl} \le \sum_{c\in C}\sum_{b\in B_s} m^F_{sb}\alpha_{scb} \qquad \forall s\in S, \omega\in\Omega \qquad (14)$$

$$\sum_{c\in C}\sum_{b\in B_s}\alpha_{scb}\,q^F_{cs} + \sum_{l\in L}\tilde{\mu}_{\omega sl}g^E_{sl} - \tilde{\zeta}^+_{\omega s} + \tilde{\zeta}^-_{\omega s} \le e^F_s \qquad \forall s\in S, \omega\in\Omega \qquad (15)$$

$$\sum_{c\in C}\sum_{b\in B_l}\beta_{lcb}\,q^R_{cl} + \sum_{k\in K}\tilde{\theta}_{\omega lk}g^E_{lk} - \tilde{\eta}^+_{\omega l} + \tilde{\eta}^-_{\omega l} \le e^R_l \qquad \forall l\in L, \omega\in\Omega \qquad (16)$$

$$\tilde{\zeta}^+_{\omega,s} \le o^F_s \qquad \forall s\in S, \omega\in\Omega \qquad (17)$$

$$\tilde{\eta}^{+}_{\omega,l} \le o^{R}_{l} \qquad \forall l \in L, \omega \in \Omega \qquad (18)$$

$$\tilde{\zeta}^{+}_{\omega,s}, \tilde{\zeta}^{-}_{\omega,s}, \tilde{\eta}^{+}_{\omega,l}, \tilde{\eta}^{-}_{\omega,l}, \tilde{\theta}_{\omega,l,k}, \tilde{\mu}_{\omega,s,l} \ge 0 \qquad \forall s \in S, l \in L, k \in K, \omega \in \Omega. \qquad (19)$$

Constraints (11) ensure that the demand processed by the logistics center is less than or equal to the customer's demand. Constraints (12)–(14) are similar to the constraints (5)–(7). Constraints (15) and (16), respectively, calculate the carbon credits transacted (purchased and sold) by producers and logistics centers by leveraging blockchain technology in scenario ω. Constraints (17) and (18) limit the carbon credits purchased by producers and logistics centers in scenario ω, respectively. Constraints (19) define the decision variables involved in the second stage.

4.3 Linearization of the objective

The nonlinear components like $\sum_{s\in S}\sum_{l\in L}\left[\mu_{sl}\left(\sum_{c\in C}\sum_{b\in B_s} k^{F}_{sb}\,\alpha_{scb}\right)\right]$ can be linearized by introducing additional variables, denoted as ε_{sbl}, and Constraints (20)–(23).

$$\varepsilon_{sbl} \le M\sum_{c\in C}\alpha_{scb} \qquad \forall s \in S, b \in B_s, l \in L \qquad (20)$$

$$\varepsilon_{sbl} \le \mu_{sl} \qquad \forall s \in S, b \in B_s, l \in L \qquad (21)$$

$$\varepsilon_{sbl} \ge \mu_{sl} - M\left(1-\sum_{c\in C}\alpha_{scb}\right) \qquad \forall s \in S, b \in B_s, l \in L \qquad (22)$$

$$\varepsilon_{sbl} \ge 0 \qquad \forall s \in S, b \in B_s, l \in L. \qquad (23)$$

Then, the above part in the objective can be reformulated as $\sum_{s\in S}\sum_{b\in B_s}\sum_{l\in L}\varepsilon_{sbl}k^{F}_{sb}$, $PL' = \sum_{s\in S}\sum_{l\in L}\mu_{sl}g^{C}_{sl} + \sum_{s\in S}\sum_{b\in B_s}\sum_{l\in L}\varepsilon_{sbl}k^{F}_{sb}$.

The second nonlinear term in the objective function $\sum_{l\in L}\sum_{k\in K}\theta_{lk}\left(\sum_{c\in C}\sum_{b\in B_l} n^{R}_{lb}\beta_{lcb}\right)$ is handled similarly. We introduce additional variables, denoted as κ_{lbk}, and the following constraints.

$$\kappa_{lbk} \le M\sum_{c\in C}\beta_{lcb} \qquad \forall l \in L, b \in B_l, k \in K \qquad (24)$$

$$\kappa_{lbk} \le \theta_{lk} \qquad \forall l \in L, b \in B_l, k \in K \qquad (25)$$

$$\kappa_{lbk} \ge \theta_{lk} - M\left(1-\sum_{c\in C}\beta_{lcb}\right) \qquad \forall l \in L, b \in B_l, k \in K \qquad (26)$$

$$\kappa_{lbk} \ge 0 \qquad \forall l \in L, b \in B_l, k \in K. \qquad (27)$$

The new cost function can then be expressed as: $LC' = \sum_{l\in L}\sum_{k\in K}\theta_{lk}g^{C}_{lk} + \sum_{l\in L}\sum_{b\in B_l}\sum_{k\in K}\kappa_{lbk}\,n^{R}_{l,b}$.

Similarly, we linearize the nonlinear part of the objective function of scenario ω in the same way. Such as $\sum_{\omega\in\Omega}\sum_{s\in S}\sum_{l\in L}\left[\tilde{\mu}_{\omega sl}\left(\sum_{c\in C}\sum_{b\in B_s} k^{F}_{sb}\,\alpha_{scb}\right)\right]$, we define the additional variables $\tilde{\varepsilon}_{\omega sbl}$ and Constraints (28)–(31).

$$\tilde{\varepsilon}_{\omega sbl} \le M\sum_{c\in C}\alpha_{scb} \qquad \forall \omega \in \Omega, s \in S, b \in B_s, l \in L \qquad (28)$$

$$\tilde{\varepsilon}_{\omega sbl} \le \tilde{\mu}_{\omega sl} \qquad \forall \omega \in \Omega, s \in S, b \in B_s, l \in L \qquad (29)$$

$$\tilde{\varepsilon}_{\omega sbl} \ge \tilde{\mu}_{\omega sl} - M\left(1-\sum_{c\in C}\alpha_{scb}\right) \qquad \forall \omega \in \Omega, s \in S, b \in B_s, l \in L \qquad (30)$$

$$\tilde{\varepsilon}_{\omega sbl} \geq 0 \qquad \forall \omega \in \Omega, s \in S, b \in B_s, l \in L. \qquad (31)$$

Then, the above part in the objective can be reformulated as $\sum_{\omega\in\Omega}\sum_{s\in S}\sum_{b\in B_s}\sum_{l\in L}\tilde{\varepsilon}_{\omega sbl}\,k^F_{sb}$, $\widetilde{PL}' = \sum_{\omega\in\Omega}\sum_{s\in S}\sum_{l\in L}\tilde{\mu}_{\omega sl}g^C_{sl} + \sum_{\omega\in\Omega}\sum_{s\in S}\sum_{b\in B_s}\sum_{l\in L}\tilde{\varepsilon}_{\omega sbl}\,k^F_{sb}$.

The second nonlinear term in the objective function $\sum_{\omega\in\Omega}\sum_{l\in L}\sum_{k\in K}\tilde{\theta}_{\omega lk}\left(\sum_{c\in C}\sum_{b\in B_l}n^R_{lb}\beta_{lcb}\right)$ is handled similarly. We introduce additional variables, denoted as $\tilde{\kappa}_{\omega lbk}$, and the following constraints.

$$\tilde{\kappa}_{\omega lbk} \leq M\sum_{c\in C}\beta_{lcb} \qquad \forall \omega \in \Omega, l \in L, b \in B_l, k \in K \qquad (32)$$

$$\tilde{\kappa}_{\omega lbk} \leq \tilde{\theta}_{\omega lk} \qquad \forall \omega \in \Omega, l \in L, b \in B_l, k \in K \qquad (33)$$

$$\tilde{\kappa}_{\omega lbk} \geq \tilde{\theta}_{\omega lk} - M(1-\sum_{c\in C}\beta_{lcb}) \qquad \forall \omega \in \Omega, l \in L, b \in B_l, k \in K \qquad (34)$$

$$\tilde{\kappa}_{\omega lbk} \geq 0 \qquad \forall \omega \in \Omega, l \in L, b \in B_l, k \in K. \qquad (35)$$

The new cost function can then be expressed as $\widetilde{LC}' = \sum_{\omega\in\Omega}\sum_{l\in L}\sum_{k\in K}\tilde{\theta}_{\omega lk}g^C_{lk} + \sum_{\omega\in\Omega}\sum_{l\in L}\sum_{b\in B_l}\sum_{k\in K}\tilde{\kappa}_{\omega lbk}\,n^R_{lb}$.

The objective function contains nonlinear terms such as $\left(\sum_{l\in L}\theta_{lk} - \sum_{l\in\in L}\tilde{\theta}_{\omega lk}\right)^+$, To linearize these expressions, we introduce additional variables $\tilde{o}^{\theta^+}_{\omega lk}, \tilde{o}^{\theta^-}_{\omega lk}$, and impose the following constraints.

$$\theta_{lk} - \tilde{\theta}_{\omega lk} = \tilde{o}^{\theta^+}_{\omega lk} - \tilde{o}^{\theta^-}_{\omega lk} \qquad \forall \omega \in \Omega, l \in L, k \in K \qquad (36)$$

$$\tilde{o}^{\theta^+}_{\omega lk}, \tilde{o}^{\theta^-}_{\omega lk} \geq 0 \qquad \forall \omega \in \Omega, l \in L, k \in K. \qquad (37)$$

Then, the objective function (10) is modified as follows.

$$Q(\boldsymbol{\theta}, \omega) = \left(\widetilde{PL}' + \widetilde{LC}'\right) + c^0\left[\sum_{\omega\in\Omega}\left(\sum_{s\in S}\left(\tilde{\zeta}^+_{\omega s} - \tilde{\zeta}^-_{\omega s}\right) + \sum_{l\in L}(\tilde{\eta}^+_{\omega l} - \tilde{\eta}^-_{\omega l})\right)\right] + \sum_{\omega\in\Omega}\sum_{k\in K}c^1\sum_{l\in L}\tilde{o}^{\theta^+}_{\omega lk}. \qquad (38)$$

Model M1 has been reformulated into an MILP model, denoted as M2.

[M2] Min $TC = FC' + PL' + LC' + \sum_{\omega\in\Omega}p_\omega\,Q(\boldsymbol{\theta}, \omega)$ (39)

subject to Constraints (2)–(9), (11)–(37).

5. Primal decomposition algorithm

A primal decomposition algorithm is designed to solve the model. Section 5.1 discusses the algorithm's framework. Sections 5.2 and 5.3 provide detailed information on how the algorithm is applied within the two-stage stochastic programming model.

5.1 Algorithmic framework

A primal decomposition algorithm decomposes a problem into a master problem and a subproblem that are generally easier to solve than the original problem. In this context, the master problem and subproblem correspond to the problems in the first and second stages.

Figure 2 shows the algorithm's framework. The algorithm employs an iterative approach, solving the

relaxation of the set-partitioning formulation for the second stage using the second-stage column generation (CG) process, detailed in Section 5.2. Concurrently, the first-stage equivalent model is solved using a first-stage CG-based algorithm, as explained in Section 5.3.

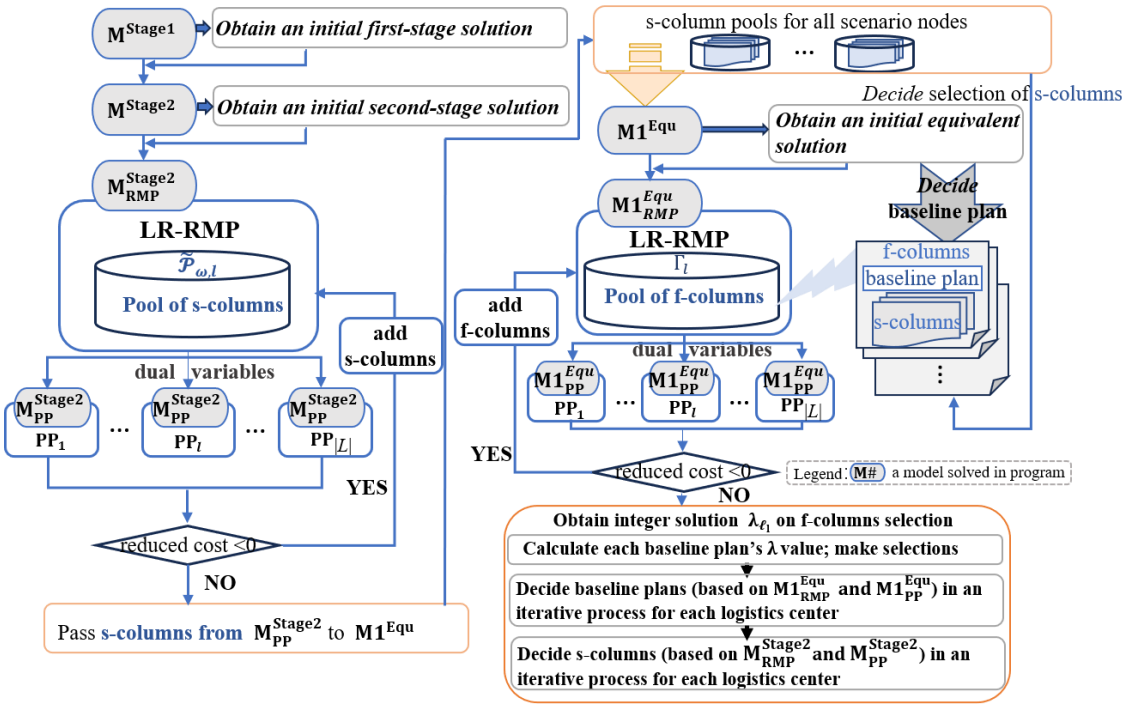

Figure 2: The overall framework of the primal decomposition algorithm

The second-stage CG procedure generates columns based on various scenarios, which are then incorporated into the first stage. Based on these generated columns, model M1 is converted into $\mathrm{M1^{Equ}}$. The first-stage CG-based algorithm is used to solve the first-stage integer programming problem, producing a feasible integer solution for the first stage. The first-stage problem is also formulated as a set-partitioning problem. To differentiate between the columns from the two stages of the problem, the columns from the first stage are referred to as f-columns, whereas those from the second stage are called s-columns. Specifically, the s-columns approximate the decisions of the second stage and are passed to the first-stage master problem. The f-columns are the columns generated in the first stage, which not only include the decisions of the first stage but also contain the selection decisions for the sub-columns corresponding to all scenarios in the second stage.

5.2 The CG for the second stage

Given any initial first-stage solution, we obtain a scenario-dependent model for each scenario ω. For simplicity and to enhance readability, we will omit the scenario index ω in the following discussion.

$$\left[\mathbf{M^{Stage2}}\right] \quad \text{Min} \quad \sum_{\omega\in\Omega} p_\omega \Big[\sum_{s\in S}\sum_{l\in L}\tilde{\mu}_{\omega sl}\big(g^C_{sl}+\sum_{c\in C}\sum_{b\in B_s}k^F_{sb}\,\alpha_{scb}\big)+\sum_{l\in L}\sum_{k\in K}\tilde{\theta}_{\omega lk}\big(g^C_{lk}+\sum_{c\in C}\sum_{b\in B_l}n^F_{lb}\,\beta_{lcb}\big)+c^0\big(\sum_{s\in S}\tilde{\zeta}_{\omega s}+\sum_{l\in L}(\tilde{\eta}^+_{\omega l}-\tilde{\eta}^-_{\omega l})\big)+\sum_{k\in K}c^1\big(\sum_{l\in L}\theta_{lk}-\sum_{l\in L}\tilde{\theta}_{\omega lk}\big)^+\Big] \quad (40)$$

subject to Constraints (11)–(19).

Then the model is expressed as the master problem (MP), denoted as $\mathrm{M}_{\mathrm{MP}}^{\mathrm{Stage2}}$, and the subproblems (PPs), denoted as $\mathrm{M}_{\mathrm{PP}}^{\mathrm{Stage2}}$, following standard column generation practices. For each logistics center l in the given scenario, we define the set $\tilde{\mathcal{P}}_l$ to include all feasible assignment plans. Each plan in $\tilde{\mathcal{P}}_l$ is indexed by p, with the associated cost denoted by $\tilde{c}_p$. We introduce a binary variable $\tilde{\lambda}_p$, $p \in \tilde{\mathcal{P}}_l$, where $\tilde{\lambda}_p$ equals one if plan p is selected for logistics center l, and zero otherwise. The parameter $\tilde{A}_k^p$ is defined to denote demand from customer k assigned to logistics center l for processing in assignment plan p. A parameter $\tilde{B}_s^p$ is defined to denote the number of products transported from producer s to logistics center l in assignment plan p. A parameter $\tilde{C}_s^p$ is defined to denote the carbon credits purchased by producer s to meet the requirements of logistics center l in assignment plan p. A parameter $\tilde{D}_s^p$ is defined to denote the carbon credits sold by producer s to meet the requirements of logistics center l in assignment plan p.

$[\mathbf{M}_{\mathbf{RMP}}^{\mathbf{Stage2}}]$ Min $\sum_{l\in L}\sum_{p\in\tilde{\mathcal{P}}_l}\tilde{c}_p\tilde{\lambda}_p$ (41)

subject to

$\sum_{p\in\tilde{\mathcal{P}}_l}\tilde{\lambda}_p = 1$ $\forall l \in L$ (42)

$\sum_{l\in L}\sum_{p\in\tilde{\mathcal{P}}_l}\tilde{A}_k^p\tilde{\lambda}_p \le \tilde{d}_{\omega k}$ $\forall k \in K$ (43)

$\sum_{l\in L}\sum_{p\in\tilde{\mathcal{P}}_l}\tilde{B}_s^p\tilde{\lambda}_p \le \sum_{c\in C}\sum_{b\in B_s} m_{sb}^F \alpha_{scb}$ $\forall s \in S$ (44)

$\sum_{c\in C}\sum_{b\in B_s}\alpha_{scb}\, q_{cs}^F + \sum_{l\in L}\sum_{p\in\tilde{\mathcal{P}}_l}\tilde{B}_s^p\, g_{sl}^E\tilde{\lambda}_p - \sum_{l\in L}\sum_{p\in\tilde{\mathcal{P}}_l}\tilde{C}_s^p\tilde{\lambda}_p + \sum_{l\in L}\sum_{p\in\tilde{\mathcal{P}}_l}\tilde{D}_s^p\tilde{\lambda}_p \le e_s^F$

$\forall s \in S$ (45)

$\sum_{l\in L}\sum_{p\in\tilde{\mathcal{P}}_l}\tilde{C}_s^p\tilde{\lambda}_p \le o_s^F$ $\forall s \in S$ (46)

$\tilde{\lambda}_p \ge 0$ $\forall l \in L, p \in \tilde{\mathcal{P}}_l.$ (47)

Objective (41) aims to minimize the total cost associated with the selected feasible plans (s-columns). Constraints (42) ensure that each logistics center l is assigned at most one feasible plan. Constraints (43) guarantee that the demand processed by logistics center l does not exceed its total demand. Constraints (44) and (45) restrict the quantity of products shipped from producer s to logistics center l that it remains within the producer's production capacity and carbon emission limits. Constraints (46) limit the maximum amount of carbon credits purchased by producer s. During each iteration, dual variables from $\mathrm{M}_{\mathrm{MP}}^{\mathrm{Stage2}}$ are used in the $\mathrm{M}_{\mathrm{PP}}^{\mathrm{Stage2}}$ to generate new s-columns. Here, π_l, ρ_k, ϱ_s, τ_s, and φ_s are dual variables for Constraints (42)–(46), respectively.

The CG procedure involves breaking down the $\mathrm{M}_{\mathrm{PP}}^{\mathrm{Stage2}}$ into $|L|$ distinct subproblems, each

corresponding to a particular logistics center. The following describes the formulation of the pricing subproblem, designed to generate feasible plans (s-columns) for each logistics center.

$$\left[\mathbf{M}_{\mathbf{PP}}^{\mathbf{Stage2}}\right] \text{Min } \tilde{c}_{\mathscr{p}} - \left[\pi_l + \sum_{k\in K} \rho_k \tilde{\theta}_{\omega k} + \sum_{s\in S} \varrho_s \tilde{\mu}_{\omega s} + \sum_{s\in S} \tau_s \left(g_{sl}^E \tilde{\mu}_{\omega s} - \tilde{\zeta}_{\omega s}^+ + \tilde{\zeta}_{\omega s}^-\right) + \right.$$

$$\left. + \sum_{s\in S} \varphi_s \tilde{\zeta}_{\omega s}^+\right] \tag{48}$$

subject to Constraints (12)–(13), (16), and (18) in·which the logistics center index l is omitted in the subscripts of the related parameters and the·variables.

$$\tilde{c}_{\mathscr{p}} = \sum_{s\in S} \tilde{\mu}_{\omega s}\left(g_s^C + \sum_{c\in C} \sum_{b\in B_s} k_{sb}^F \alpha_{scb}\right) + \sum_{k\in K} \tilde{\theta}_{\omega k}\left[g_k^C + \sum_{c\in C} \sum_{b\in B_l} n_b^R \beta_{cb}\right] +$$

$$c^0\left[\sum_{s\in S}(\tilde{\zeta}_{\omega s}^+ - \tilde{\zeta}_{\omega s}^-) + (\tilde{\eta}_{\omega}^+ - \tilde{\eta}_{\omega}^-)\right] + c^1 \sum_{k\in K}\left(\theta_k - \tilde{\theta}_{\omega k}\right)^+ \tag{49}$$

Objective (48) aims to minimize the reduced cost associated with the optimal assignment plan. Constraint (49) calculates the total cost of the logistics center plan.

5.3 The CG for the first stage

We developed a model $\mathrm{M1}^{\mathrm{Equ}}$ equivalent to the original model $\mathrm{M1}$, and defined the Restricted Master Problem (RMP) and Pricing Problem (PP) for this model. Note that each column of the equivalent model consists of a series of sub-columns (i.e., columns from the first-stage CG), with the number of sub-columns corresponding to the number of second-stage scenarios. Additionally, new parameters and decision variables were defined.

Newly defined parameters and sets:

$\tilde{\mathcal{P}}_{\omega l}$ represent the collection of all sub-columns for logistics center l in scenario ω, indexed by $\mathscr{p}$;

$\tilde{r}_{\omega lkp}$ in the sub-column indexed by $\mathscr{p}$ within scenario ω, the demand of customer k handled by logistics center l; $\omega \in \Omega,\ \mathscr{p} \in \tilde{\mathcal{P}}_{\omega l}$;

$\tilde{j}_{\omega slp}$ in the sub-column indexed by $\mathscr{p}$ within scenario ω, the number of products transported from producer s to logistics center l, $\omega \in \Omega,\ \mathscr{p} \in \tilde{\mathcal{P}}_{\omega l}$;

$\tilde{z}_{\omega slp}^+$ in the sub-column indexed by $\mathscr{p}$ within scenario ω, the carbon credits purchased by producer s to meet the transportation needs of logistics center l, $\omega \in \Omega,\ \mathscr{p} \in \tilde{\mathcal{P}}_{\omega l}$;

$\tilde{z}_{\omega slp}^-$ in the sub-column indexed by $\mathscr{p}$ within scenario ω, the carbon credits sold by producer s to meet the transportation needs of logistics center l, $\omega \in \Omega,\ \mathscr{p} \in \tilde{\mathcal{P}}_{\omega l}$;

$\tilde{w}_{\omega lp}^+$ in the sub-column indexed by $\mathscr{p}$ within scenario ω, the carbon credits purchased by logistics center l, $\omega \in \Omega,\ \mathscr{p} \in \tilde{\mathcal{P}}_{\omega l}$;

$\tilde{w}_{\omega lp}^-$ within the sub-column $\mathscr{p}$ within scenario ω, the carbon credits sold by logistics center l, $\omega \in \Omega,\ \mathscr{p} \in \tilde{\mathcal{P}}_{\omega l}$.

Newly defined variables:

$\tilde{\chi}_{\omega lp}$ binary; equals one when sub-column p is chosen for logistics center l in scenario ω, $\omega \in \Omega$, $p \in \tilde{\mathcal{P}}_{\omega l}$.

$\tilde{\vartheta}_{\omega lp}$ cost associated with sub-column p for logistics center l in scenario ω,

Then, we formulate $\mathrm{M1}^{\mathrm{Equ}}$ as follows. Note that in order to adapt the CG algorithm, a new parameter α'_{scbl} is defined in the $\mathrm{M1}^{\mathrm{Equ}}$ to the decision variable α_{scb}.

$$[\mathbf{M1^{Equ}}] \ \text{Min} \ FC + PL + LC + \sum_{\omega\in\Omega}\sum_{l\in L}\sum_{p\in\tilde{\mathcal{P}}_{\omega l}} p_\omega \tilde{\vartheta}_{\omega lp}\tilde{\chi}_{\omega lp} \quad (50)$$

subject to Constraints (2)–(9).

$$\sum_{p\in\tilde{\mathcal{P}}_{\omega l}} \tilde{\chi}_{\omega lp} = 1 \qquad \forall l \in L, \omega \in \Omega \quad (51)$$

$$\sum_{l\in L}\sum_{p\in\tilde{\mathcal{P}}_{\omega l}} \tilde{r}_{\omega lkp}\tilde{\chi}_{\omega lp} \le \tilde{d}_{\omega k} \qquad \forall k \in K, \omega \in \Omega \quad (52)$$

$$\sum_{l\in L}\sum_{p\in\tilde{\mathcal{P}}_{\omega l}} \tilde{j}_{\omega slp}\tilde{\chi}_{\omega lp} \le \sum_{c\in C}\sum_{b\in B_s} m^F_{sb}\alpha_{scb} \qquad \forall s \in S, \omega \in \Omega \quad (53)$$

$$\sum_{c\in C}\sum_{b\in B_s} \alpha_{scb}\, q^F_{cs} + \sum_{l\in L}\sum_{p\in\tilde{\mathcal{P}}_{\omega l}} \tilde{j}_{\omega slp} g^E_{sl}\tilde{\chi}_{\omega lp} - \sum_{l\in L}\sum_{p\in\tilde{\mathcal{P}}_{\omega l}} \tilde{z}^+_{\omega slp}\,\tilde{\chi}_{\omega lp} + \sum_{l\in L}\sum_{p\in\tilde{\mathcal{P}}_{\omega l}} \tilde{z}^-_{\omega slp}\tilde{\chi}_{\omega lp} \le e^F_s \qquad \forall s \in S, \omega \in \Omega \quad (54)$$

$$\sum_{l\in L}\sum_{p\in\tilde{\mathcal{P}}_{\omega l}} \tilde{z}^+_{\omega slp}\tilde{\chi}_{\omega lp} \le o^F_s \qquad \forall s \in S, \omega \in \Omega \quad (55)$$

$$\alpha'_{scbl} = \alpha_{scb} \qquad \forall s \in S, c \in C, b \in B, l \in L \quad (56)$$

$$\tilde{\vartheta}_{\omega lp} = \sum_{s\in S}\tilde{j}_{\omega slp}\left(g^C_{sl} + \sum_{c\in C}\sum_{b\in B_s} k^F_{sb}\,\alpha'_{scbl}\right) + \sum_{k\in K}\tilde{r}_{\omega lkp}\left(g^C_{lk} + \sum_{c\in C}\sum_{b\in B_l} n^R_b\,\beta_{lcb}\right) + c^0\left[\sum_{s\in S}\left(\tilde{z}^+_{\omega slp} - \tilde{z}^-_{\omega slp}\right) + \left(\tilde{w}^+_{\omega lp} - \tilde{w}^-_{\omega lp}\right)\right] + \sum_{k\in K} c^1\left(\theta_{lk} - \tilde{r}_{\omega lkp}\right)^+ \qquad \forall \omega \in \Omega, l \in L, p \in \tilde{\mathcal{P}}_{\omega l} \quad (57)$$

$$\tilde{\chi}_{\omega lp}, \alpha_{scb}, \alpha'_{scbl}, \beta_{lcb} \in \{0,1\} \qquad \forall \omega \in \Omega, l \in L, p \in \tilde{\mathcal{P}}_{\omega l}, s \in S, c \in C, b \in B \quad (58)$$

$$\theta_{lk}, \mu_{sl} \ge 0 \qquad \forall s \in S, l \in L, k \in K. \quad (59)$$

The nonlinear components like $\sum_{\omega\in\Omega}\sum_{l\in L}\sum_{p\in\tilde{\mathcal{P}}_{\omega l}} p_\omega \tilde{\vartheta}_{\omega lp}\tilde{\chi}_{\omega lp}$ can be linearized by introducing additional variables, denoted as $\psi_{\omega lp}$. To achieve this, we impose a new set of constraints.

$$\psi_{\omega lp} \le \tilde{\vartheta}_{\omega lp} \qquad \forall \omega \in \Omega, l \in L, p \in P \quad (60)$$

$$\psi_{\omega lp} \le M\tilde{\chi}_{\omega lp} \qquad \forall \omega \in \Omega, l \in L, p \in P \quad (61)$$

$$\psi_{\omega lp} \ge \tilde{\vartheta}_{\omega lp} - M(1 - \tilde{\chi}_{\omega lp}) \qquad \forall \omega \in \Omega, l \in L, p \in P \quad (62)$$

With the newly introduced variables and constraints, model $\mathrm{M1}^{\mathrm{Equ}}$ is reformulated into an MILP model.

$$[\mathbf{M1^{Equ}}] \ \text{Min} \ FC + PL + LC + \sum_{\omega\in\Omega}\sum_{l\in L}\sum_{p\in\tilde{\mathcal{P}}_{\omega l}} p_\omega\,\psi_{\omega lp} \quad (63)$$

subject to Constraints (2)–(9), (51)–(59), (60)–(62).

By utilizing the sub-columns from the sets $\tilde{\mathcal{P}}_{\omega l}$, second-stage decisions across all scenarios are

incorporated into the first-stage master problem via Constraints (56) to (64). We then restructure the equivalent model $\mathrm{M1}^{\mathrm{Equ}}$ into a set covering model. In our approach, the algorithm iterates between solving $\mathrm{M1}^{\mathrm{Equ}}$ to obtain a valid first-stage solution (i.e., a baseline schedule), and generating new s-columns from the second stage by applying the second-stage column generation process in $\mathrm{M}^{\mathrm{Stage2}}$. The complete set of all feasible assignment plans for logistics center l is represented as Γ_l, where each individual assignment plan, indexed by ℓ_l, corresponds to a column. A binary decision variable λ_{ℓ_l} is assigned to each column, taking the value of one if column ℓ_l is selected for logistics center l, and zero otherwise. The cost for each column ℓ_l is denoted by c_{ℓ_l}. A parameter α'_{scbl} is defined to denote producer s sited in a location with a level of emission control c and a level of production capacity b for the logistics center l. A parameter $G_k^{\ell_l}$ is defined to denote demand from customer k assigned to logistics center l in column ℓ_l. A parameter $U_s^{\ell_l}$ is defined to denote the number of products transported from producer s to logistics center l in column ℓ_l. A parameter $L_{\omega p}^{\ell_l}$ is set to one when plan $p \in \tilde{\mathcal{P}}_{\omega l}$ is chosen in column ℓ_l. A parameter $H_{scb}^{\ell_l}$ is defined to equals one if producer s sited in a location with a level of emission control c and a level of production capacity b for the logistics center l in column ℓ_l.

$[\mathbf{M1}_{\boldsymbol{RMP}}^{\boldsymbol{Equ}}]$ Min $\sum_{l\in L}\sum_{\ell_l\in\Gamma_l} c_{\ell_l}\lambda_{\ell_l}$ (64)

subject to

$\sum_{\ell_l\in\Gamma_l}\lambda_{\ell_l} = 1$ $\forall l \in L$ (65)

$\sum_{c\in C}\sum_{b\in B_s}\alpha_{scb} \le 1$` $\forall s \in S$ (66)

$\sum_{l\in L}\sum_{\ell_l\in\Gamma_l}\lambda_{\ell_l} G_k^{\ell_l} \ge d_k$ $\forall k \in K$ (67)

$\sum_{l\in L}\sum_{\ell_l\in\Gamma_l}\lambda_{\ell_l} U_s^{\ell_l} \le \sum_{c\in C}\sum_{b\in B_s} m_{sb}^F \alpha_{scb}$ $\forall s \in S$ (68)

$\sum_{l\in L}\sum_{p\in\tilde{\mathcal{P}}_{\omega l}} \tilde{r}_{\omega lkp} L_{\omega p}^{\ell_l} \sum_{\ell_l\in\Gamma_l}\lambda_{\ell_l} \le \tilde{d}_{\omega k}$ $\forall k \in K, \omega \in \Omega$ (69)

$\sum_{l\in L}\sum_{p\in\tilde{\mathcal{P}}_{\omega l}} \tilde{j}_{\omega slp} L_{\omega p}^{\ell_l} \sum_{\ell_l\in\Gamma_l}\lambda_{\ell_l} \le \sum_{c\in C}\sum_{b\in B_s} m_{sb}^F \alpha_{scb}$ $\forall s \in S, \omega \in \Omega$ (70)

$\sum_{c\in C}\sum_{b\in B_s}\alpha_{scb}\, q_{cs}^F + \sum_{l\in L}\sum_{p\in\tilde{\mathcal{P}}_{\omega l}} \tilde{j}_{\omega slp} g_{sl}^E L_{\omega p}^{\ell_l} \sum_{\ell_l\in\Gamma_l}\lambda_{\ell_l} - \sum_{l\in L}\sum_{p\in\tilde{\mathcal{P}}_{\omega l}} \tilde{z}_{\omega sp}^{+} L_{\omega p}^{\ell_l} \sum_{\ell_l\in\Gamma_l}\lambda_{\ell_l} +$
$\sum_{l\in L}\sum_{p\in\tilde{\mathcal{P}}_{\omega l}} \tilde{z}_{\omega sp}^{-} L_{\omega p}^{\ell_l} \sum_{\ell_l\in\Gamma_l}\lambda_{\ell_l} \le e_s^F$ $\forall s \in S, \omega \in \Omega$ (71)

$\sum_{l\in L}\sum_{p\in\tilde{\mathcal{P}}_{\omega l}} \tilde{z}_{\omega sp}^{+} L_{\omega p}^{\ell_l} \sum_{\ell_l\in\Gamma_l}\lambda_{\ell_l} \le o_s^F$ $\forall s \in S, \omega \in \Omega$ (72)

$H_{scb}^{\ell_l} \sum_{\ell_l\in\Gamma_l}\lambda_{\ell_l} = \alpha_{scb}$ $\forall s \in S, c \in C, b \in B, l \in L$ (73)

$\alpha_{scb} \in \{0,1\}$ $\forall s \in S, c \in C, b \in B$ (74)

$\lambda_{\ell_l} \ge 0$ $\forall l \in L.$ (75)

During each iteration, the dual variables from $\mathrm{M1}_{\boldsymbol{MP}}^{\boldsymbol{Equ}}$ are passed to the subproblem (PP) to generate new columns. Here, y_l, u_k, ϖ_s, $\varsigma_{\omega k}$, $\sigma_{\omega s}$, $\xi_{\omega s}$, $\iota_{\omega s}$ and $\eth_{scbl}$ are dual variables for Constraints (65) and Constraints (67)–(73), respectively.

The PP is split into $|L|$ separate pricing subproblems, with each one assigned to a specific logistics center. The subproblem for generating f-columns for logistics center l is denoted as PP_l and formulated as the $\mathrm{M1}_{PP}^{Equ}$. The new variables defined for the PP are as follows.

$\tilde{\chi}_{\omega p}$ binary; equals one when sub-column $\mathscr{p}$ is chosen for logistics center l in scenario ω, $\omega \in \Omega, \mathscr{p} \in \tilde{\mathcal{P}}_{\omega l}$;

$\tilde{\vartheta}_{\omega \mathscr{p}}$ cost associated with sub-column $\mathscr{p}$ for logistics center l in scenario $\omega, \omega \in \Omega, \mathscr{p} \in \tilde{\mathcal{P}}_{\omega l}$.

Since the variables mentioned are utilized in the pricing subproblem for a single logistics center, the index l is omitted from the variable subscripts for simplicity.

$$\left[\mathbf{M1}_{\boldsymbol{PP}}^{\boldsymbol{Equ}}\right] \quad \text{Min} \quad c_{\ell_l} - (y_l + \sum_{k\in K} \theta_k u_k + \sum_{s\in S} \mu_s \varpi_s + \sum_{\omega\in\Omega} \sum_{\mathscr{p}\in\tilde{\mathcal{P}}_{\omega l}} \sum_{k\in K} \tilde{r}_{\omega k p} \tilde{\chi}_{\omega p} \varsigma_{\omega k} + \sum_{\omega\in\Omega} \sum_{\mathscr{p}\in\tilde{\mathcal{P}}_{\omega l}} \sum_{s\in S} \tilde{J}_{\omega s p} \tilde{\chi}_{\omega p} \sigma_{\omega s} + \sum_{\omega\in\Omega} \sum_{\mathscr{p}\in\tilde{\mathcal{P}}_{\omega l}} \sum_{s\in S} \xi_{\omega s} \left(\tilde{J}_{\omega s p} g_s^E \tilde{\chi}_{\omega p} - \tilde{z}_{\omega s p}^{+} \tilde{\chi}_{\omega p} + \tilde{z}_{\omega s p}^{-} \tilde{\chi}_{\omega p}\right) + \sum_{\omega\in\Omega} \sum_{\mathscr{p}\in\tilde{\mathcal{P}}_{\omega l}} \sum_{s\in S} \iota_{\omega s} \tilde{z}_{\omega s p}^{+} \tilde{\chi}_{\omega p} + \sum_{s\in S} \sum_{c\in C} \sum_{b\in B_s} \eth_{scb} \alpha'_{scb}) \tag{76}$$

subject to Constraints (3), (5), (6), (51), (57) and (58)–(59) in·which the logistics center index l is omitted in the subscripts of the related parameters and the·variables.

$$c_{\ell_l} = \sum_{s\in S} \sum_{c\in C} \sum_{b\in B_s} f_{scb}^F / L \alpha'_{scb} + \sum_{c\in C} \sum_{b\in B_l} f_{cb} \beta_{cb} + \sum_{s\in S} \mu_s \left(g_s^C + \sum_{c\in C} \sum_{b\in B_s} k_{sb}^F \alpha'_{scb}\right) + \sum_{k\in K} \theta_k \left(g_k^C + \sum_{c\in C} \sum_{b\in B_l} n_b^F \beta_{cb}\right) + \sum_{\omega\in\Omega} \sum_{\mathscr{p}\in\tilde{\mathcal{P}}_{\omega l}} p_\omega \tilde{\vartheta}_{\omega \mathscr{p}} \tilde{\chi}_{\omega p} \tag{77}$$

The objective (76) aims to minimize the cost of the assignment plan. Constraint (77) calculates the cost of the assignment plan for the logistics center.

6. Numerical experiments

To assess the effectiveness of the proposed model and the efficiency of the primal decomposition algorithm, numerical experiments were performed on a workstation equipped with an Intel Xeon Gold 5218R CPU running at 2.10 GHz and 32 GB of RAM. The models and algorithms were implemented using C# in Visual Studio 2022, utilizing the ILOG CPLEX 22.1.0 solver. Each instance was allocated a maximum of 3,600 seconds for computation.

6.1 Experimental settings

We use SAIC as a case study, utilizing data from the organization to conduct numerical experiments to validate our model and algorithm. SAIC is one of the largest automobile manufacturers in China. It is headquartered in Shanghai and has multiple production bases and logistics centers in provinces such

as Shanghai, Shandong, Hubei, Fujian, and Liaoning. These facilities include various automobile manufacturing and assembly plants, forming a complex and extensive supply chain network. In recent years, SAIC has actively promoted green manufacturing and sustainable development by implementing measures to reduce carbon emissions and achieve environmentally friendly production practices. Figure 3 illustrates the geographic distribution of SAIC's customer segments and the potential candidate sites for their production facilities and logistics centers. In the figure, larger circular icons (representing customer segments) indicate higher local customer demand. The test data are extrapolated from historical operational records. Appendix A comprehensively describes the primary input parameters used in the mathematical model.

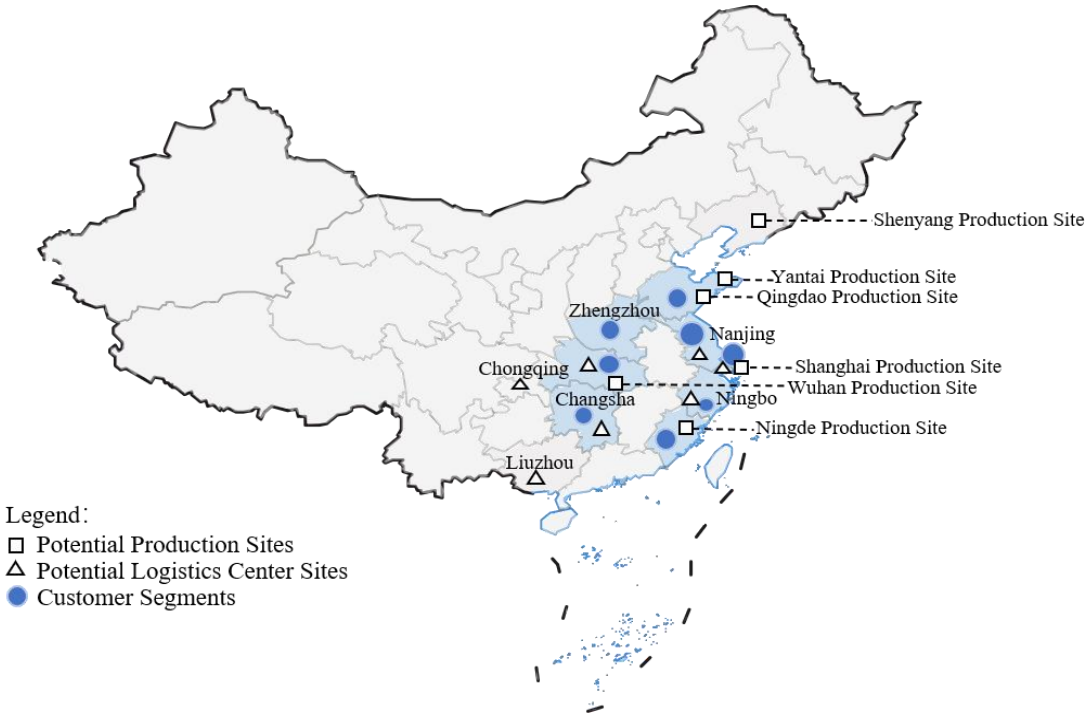

Figure 3: Layout of potential facility locations and customer positions

We create 4 experimental groups, and the largest ISG has 100 uncertain scenarios. Table 1 details the specific settings for the set of instances.

Table 1: Scale of instance groups employed in the experiments

Group ID	No. of producers	No. of logistics centers	No. of customers	No. of scenarios
ISG1	2	3	3	5
ISG2	5	7	7	25
ISG3	6	8	8	50
ISG4	6	8	8	100

6.2 Solution quality

We begin by evaluating small–scale instances to compare the optimal performance of CPLEX, our proposed primal decomposition algorithm, and a lower bound (LB) that relaxes the binary variables β_{lcb}. The results from testing randomly generated instances in the ISG1 and ISG2 groups, detailed in

Table 2, show that CPLEX can only handle the initial set of small-scale instances, ISG1, which consists of five scenarios. The computation time the solver requires for ISG1 is slightly less than our algorithm requires. However, as the problem size increases, the computation time required by CPLEX rises sharply. As indicated by the gap value (GAP_2) in Table 2, our approach achieves optimal solutions consistently (with an average deviation of 0 from the optimal solutions), demonstrating its reliability.

Table 2: Performance of the algorithm on small-scale instances

Instances		CPLEX		LB	Primal decomposition algorithm			
Group	ID	F_{CPLEX}	t_{CPLEX}	F_{LB}	F_{DCG}	t_{DCG}	GAP_1	GAP_2
ISG1	1-1	70632	0.33	63,252	70,632	9.06	11.67%	0.00%
	1-2	65504	0.25	55,608	65,504	6.67	17.80%	0.00%
	1-3	62702	0.25	53,639	62,702	7.06	16.90%	0.00%
	1-4	80977	0.47	68,217	80,977	9.19	18.70%	0.00%
	1-5	67581	0.25	52,813	67,582	8.50	27.96%	0.00%
ISG2	2-1	—	—	185,153	206,832	50.70	11.71%	—
	2-2	—	—	170,759	179,058	32.58	4.86%	—
	2-3	—	—	170,211	190,536	48.78	11.94%	—
	2-4	—	—	139,192	169,600	39.83	21.85%	—
	2-5	—	—	128,427	150,624	60.02	17.28%	—
Average							16.07%	0.00%

Notes: (1) F_{CPLEX}, F_{LB} and F_{DCG} denote the objective values of the solutions obtained from CPLEX, the LB, and the primal decomposition algorithm, respectively. The units of these objective values are in ten thousand RMB. (2) t_{CPLEX} and t_{DCG} represent the computation times, in seconds, for the CPLEX solver and the primal decomposition algorithm, respectively. (3) $Gap_1 = (F_{DCG} - F_{LB})/F_{LB}$; $Gap_2 = (F_{CPLEX} - F_{DCG})/F_{CPLXE}$. (4) The symbol "—" indicates that CPLEX was unable to solve the instances within the 3600-second time limit.

The CPLEX solver is not effective at solving large-scale instances. To further demonstrate the efficacy of our algorithm, we perform tests on large-scale instances and compare the results of the primal decomposition algorithm against those of the LB. As shown in Table 3, the average deviation (GAP3) between the results of our algorithm and the LB is around 11.10%, similar to the average deviation of 16.07% observed for smaller instances. CPLEX fails to solve any test cases in ISG2, ISG3, and ISG4 within 1 hour. In contrast, the primal decomposition algorithm obtains solutions for each instance within 5 minutes, demonstrating its effectiveness in large-scale instances.

Table 3: Performance of the algorithm on large-scale instances

Instances		LB	Primal decomposition algorithm		
Group	ID	F_{LB}	F_{DCG}	t_{DCG}	GAP_1
ISG3	3-1	203,301	231,616	116.65	13.93%
	3-2	192,416	221,088	96.10	14.90%
	3-3	185,317	215,006	77.78	16.02%
	3-4	194,579	225,643	72.63	15.96%
	3-5	187,398	217,529	88.89	16.08%
ISG4	4-1	327,690	347,617	186.47	6.08%
	4-2	236,647	257,420	266.78	8.78%
	4-3	279,510	300,284	236.87	7.43%
	4-4	387,364	412,762	299.85	6.56%

	4-5	330,424	347,738	245.64	5.24%
Average					11.10%

Notes: (1) F_{LB} and F_{DCG} denote the objective values of the solutions obtained from LB and primal decomposition algorithm, respectively. The units of these objective values are in ten thousand RMB. (2) t_{DCG} represents the computation times, in seconds, for primal decomposition algorithm. (3) $Gap_1 = (F_{DCG} - F_{LB})/F_{LB}$.

6.3 Benefits of stochastic programming

In this paper, we adopt a stochastic programming approach to address uncertainty in customer demand in supply chains. To demonstrate the advantages of this method, we define three distinct decision-making approaches and conduct a series of experiments to compare them.

Method 1: This method employs a stochastic model (i.e., the proposed model M1) to optimize the problem under various uncertainty scenarios. The resulting objective value is denoted by Z_1.

Method 2: This method uses a deterministic model. The model is constructed based on the original model but operates under a single scenario. In this scenario, each random parameter (such as customer demand) is replaced with its expected value, the average across all scenarios. The first stage of the problem is solved under this deterministic setup, and the second stage is then solved based on the solution from the first stage. The objective value of this method is denoted as Z_2.

Method 3: This approach addresses the problem by solving a set of deterministic models, each representing a specific scenario derived from actual customer demand. Following the resolution of these models, the average of their objective values is calculated and referred to as Z_3.

Table 4: Experimental results on the benefits of stochastic programming

Instances		Z_1	Z_2	Z_3	gap_{stocha}	gap_{info}
Group	ID					
ISG2	2-6	380,048	396,792	377,350	4.41%	0.71%
	2-7	297,297	312,561	294,245	5.13%	1.03%
	2-8	559,387	588,776	548,485	5.25%	1.95%
	2-9	345,116	366,580	339,801	6.22%	1.54%
	2-10	441,107	470,506	428,758	6.67%	2.80%
	2-11	211,091	226,844	201,898	7.46%	4.35%
	2-12	341,569	368,120	334,157	7.77%	2.17%
	2-13	107,596	120,786	104,115	12.26%	3.24%
	2-14	233,204	262,167	226,351	12.42%	2.94%
	2-15	126,630	143,646	123,514	13.44%	2.46%
Average					8.10%	2.32%

Notes: (1) The units of these objective values are in ten thousand RMB. (2) $gap_{stocha} = (Z_2 - Z_1)/Z_1$ and $gap_{info} = (Z_3 - Z_1)/Z_1$.

Z_1 is generally less than or equal to Z_2, and the disparity between these two values represents the cost associated with disregarding uncertainty in the decision-making process. This difference is referred to as the *value of the stochastic solution*, $Val_{stocha} = Z_2 - Z_1$, and it quantifies the impact of ignoring stochastic factors. Method 3 is often impractical in real-world scenarios due to the challenges inherent in accurately predicting customer demand. In such cases, Z_3 is often considered as a lower bound for

Z_1. The disparity between Z_1 and Z_3 is referred to as the *value of perfect information*, $Val_{info} = Z_3 - Z_1$, and it quantifies the impact of uncertainty and the potential benefits of accurate information. Therefore, it is critical to incorporate stochastic factors into the initial stages of scheduling methods. The results of the comparative experiments are summarized in Table 4. In the table, the percentages of Val_{stocha} and Val_{info} relative to the target value of the original model are represented by gap_{stocha} and gap_{info}, respectively. These results underscore the importance of considering uncertainty during the optimization process.

6.4 Managerial insights from sensitivity analysis

We conduct several experiments to obtain insights for managing sustainability in supply chains.

(1) Sensitivity analysis of customer demand

We perform a series of sensitivity analyses to assess how various levels of certain and uncertain demand affect the overall cost of the supply chain. These analyses are conducted using the ISG3 scale, and the findings are illustrated in Figure 4.

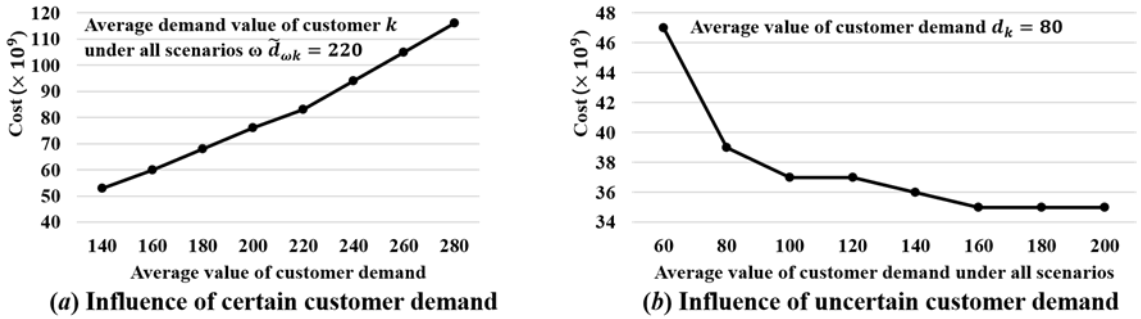

(*a*) **Influence of certain customer demand** (*b*) **Influence of uncertain customer demand**

Figure 4: Sensitivity analysis of customer demand

Figure 4(*a*) illustrates that total supply chain costs increase as the average certain customer demand (d_k) grows along the horizontal axis when the average uncertain customer demand across all uncertainty scenarios ($\tilde{d}_{\omega k}$) is fixed at 220. The term "average customer demand" refers to "expected customer demand", typically derived from historical data or forecasts that provide a consistent value. In our model, this demand represents a scenario where uncertainty is not considered. "Average uncertain customer demand" refers to the average demand across all uncertain scenarios. Considering potential variations or fluctuations in customer demand, we use the average value to represent the unpredictability of demand under such conditions. Notably, when certain demand reaches the same level as uncertain demand (i.e., $\tilde{d}_{\omega k} = 220$), the increase in costs becomes more pronounced. Our mathematical model and real-world observations can explain this phenomenon: certain demand represents information known to supply chain members and primarily influences first-stage decisions, such as facility location and capacity planning. An increase in demand leads to higher production and transportation

requirements, and existing capacity may become insufficient, necessitating additional facilities and increasing costs. When first-stage certain demand surpasses second-stage uncertain demand, the actual uncertain demand handled by the supply chain is less than initially planned, a scenario commonly observed in real-world supply chains. For example, due to market fluctuations and emission reduction requirements, the actual customer demand handled by the supply chain may be lower than previously estimated. In such cases, the unmet demand causes the supply chain to incur penalties, which are reflected as additional costs in our model, resulting in a more significant increase in cost. Therefore, supply chain members should strive to accurately forecast uncertain demand and mitigate the impact of demand fluctuations on the supply chain to minimize costs.

Figure 4(b) shows that when the average certain customer demand (d_k) is fixed at 80, the total supply chain costs decrease as the average uncertain customer demand across all scenarios of uncertainty ($\tilde{d}_{\omega k}$) increases along the horizontal axis, eventually stabilizing. Consistent with the analysis depicted in Figure 4(a), when uncertain demand is lower than certain demand (in the 60-80 range on the horizontal axis of Figure 4(b)), the total supply chain costs fluctuate significantly. The total supply chain costs decline most sharply when uncertain demand is less than and approaches certain demand ($d_k = 80$). As uncertain demand exceeds certain demand, the cost decreases, but at a slower rate, until it stabilizes. This is because handling higher uncertain demand reduces penalty costs. Still, carbon quotas and carbon credit limits prevent the supply chain from meeting demand indefinitely, causing costs to reach a lower bound. Therefore, supply chain members should strive to meet demand as much as possible while considering emission reduction requirements to avoid overproduction.

(2) Sensitivity analysis on the ratio of carbon quota for producers and logistics center

Secondly, the influence of the ratio of the carbon quota of producers to that of logistics centers on the total cost of the supply chain is investigated. To explore differences in the decision-making outcomes at different scales, we conduct experiments using examples of both small-scale and large-scale supply chains. The results are shown in Figure 5.

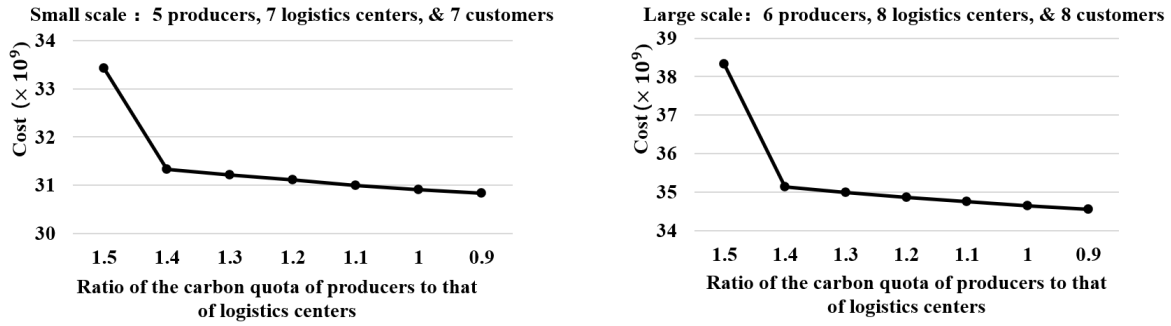

Figure 5: Sensitivity analysis of the ratio of the carbon quota of producers to that of logistics centers

As shown in Figure 5, total supply chain costs decrease as the carbon quota ratio between producers

and logistics centers decreases in both small-scale and large-scale scenarios. In both cases, the most significant cost reduction occurs when the ratio is 1.4, after which the cost reduction trend gradually slows as the ratio continues to decrease. This is because a smaller ratio implies a relatively larger carbon quota for logistics centers than producers, allowing logistics centers to sell more carbon credits, thereby reducing costs.

In practical terms, logistics centers, which serve as transportation hubs connecting producers and customers, tend to emit more carbon dioxide during transportation than producers. Moreover, transportation-related carbon emissions constitute a significant portion of the total emissions across the supply chain. This highlights the importance of strategically allocating carbon quotas, ensuring that logistics centers, often the largest emitters, have sufficient quotas to avoid excessive carbon credit costs.

Therefore, supply chain managers should prioritize minimizing distances between supply chain nodes to reduce transportation-related emissions in real-world scenarios. Additionally, efforts should be made to allocate more carbon quota to logistics centers to optimize cost-efficiency and carbon management.

(3) Sensitivity analysis of minimum production capacity

Finally, we examine the impact of producers' minimum production capacity levels on the total supply chain costs. To explore differences in the decision-making outcomes across different scales, we conduct experiments using examples of both small-scale and large-scale supply chains. The results are shown in Figure 6.

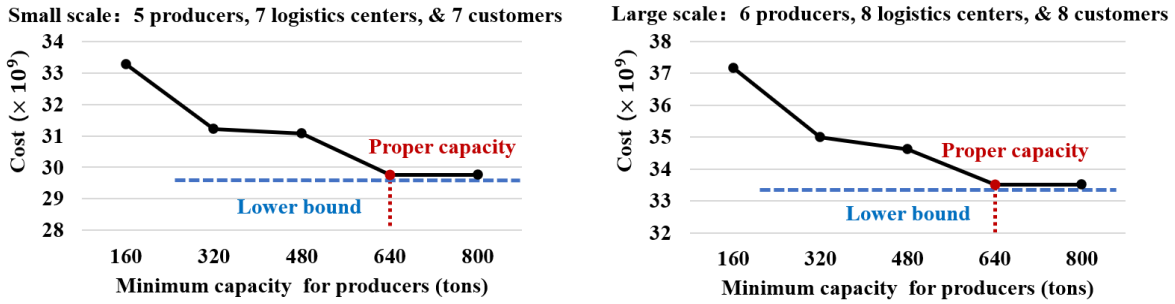

Figure 6: Sensitivity analysis of the minimum level of producers' capacity

As shown in the figure, regardless of scale, total supply chain costs decrease as producers' minimum production capacity increases, eventually reaching a lower bound. This is because higher minimum production capacity reduces the number of producers required to meet fixed demand, thereby lowering initial facility location and operational costs. Additionally, as more demand is satisfied, penalty costs decrease, leading to a corresponding reduction in total costs.

However, when the minimum production capacity reaches a certain threshold (e.g., 640 in Figure 6), further capacity increases no longer reduce costs. This is because the existing capacity is sufficient to meet demand, and additional production would only result in increased inventory and transportation

costs. In our model, increased production also raises the processing volume at logistics centers, thereby increasing carbon emissions. Producers and logistics centers may limit production to reduce carbon emissions and related trading costs, leading to idle capacity and stabilized costs.

From a managerial perspective, this indicates the importance of evaluating appropriate capacity levels when selecting production equipment. Blindly pursuing higher capacity is not advisable. Instead, producers should invest in energy-efficient and environmentally friendly equipment to avoid the waste and cost increases associated with overcapacity, which could impact the sustainability and profitability of the supply chain.

6.5 Benefits of blockchain

A key contribution of this study is integrating blockchain technology into the design of sustainable supply chain networks, along with the formulation of smart contract rules to limit carbon emissions and optimize carbon trading decisions. The advantages of blockchain are evaluated by comparing the proposed model to one that does not incorporate blockchain technology. This evaluation is detailed in Appendix B. The results, illustrated in Figure 7, indicate that blockchain technology reduces the total cost of the supply chain, as quantified by the gap (%) values. The results also demonstrate that when demand (d_k in Figure 7) is higher, the benefits of blockchain, as indicated by the gap (%) values, are greater. The benefits become more pronounced as the supply chain's scale grows. These findings demonstrate that the blockchain-enabled model offers substantial advantages in carbon emission control, cost efficiency, and operational flexibility. Specifically, the blockchain-enabled model more effectively maintains emissions within allocated limits, achieves lower overall costs through automated carbon trading, and responds more efficiently to demand fluctuations than the conventional model.

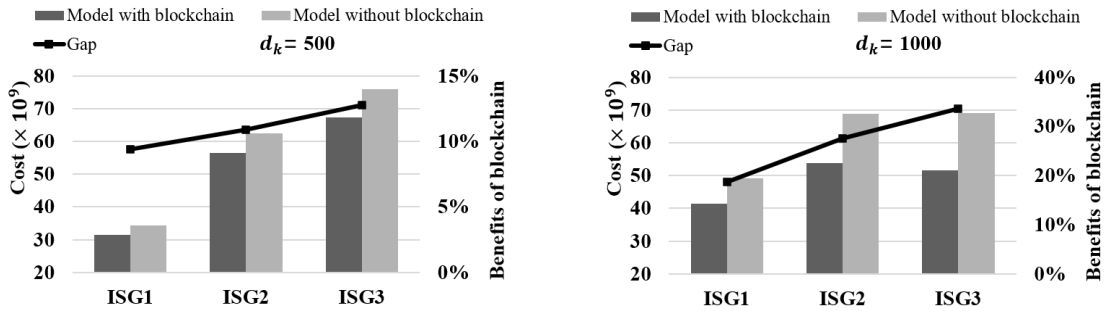

Figure 7: Benefits of considering blockchain

6.6 Robustness of the model against carbon credit price deviations

The carbon credit prices in this study are estimated based on data from the National Carbon Trading Market Information Network (https://www.cets.org.cn/). However, carbon credit prices fluctuate significantly daily, and market volatility may lead to inaccuracies in the estimates. We thus conduct a

robustness test to evaluate the model's robustness against carbon credit price fluctuations. As shown in Figure 8, when carbon credit prices exceed the estimated values by 10%, 15%, and up to 30%, the total cost (i.e., OBJ) calculated based on the estimates differs by no more than 1% from the optimal results obtained using actual parameters. This confirms the robustness of the proposed model under carbon credit price fluctuations.

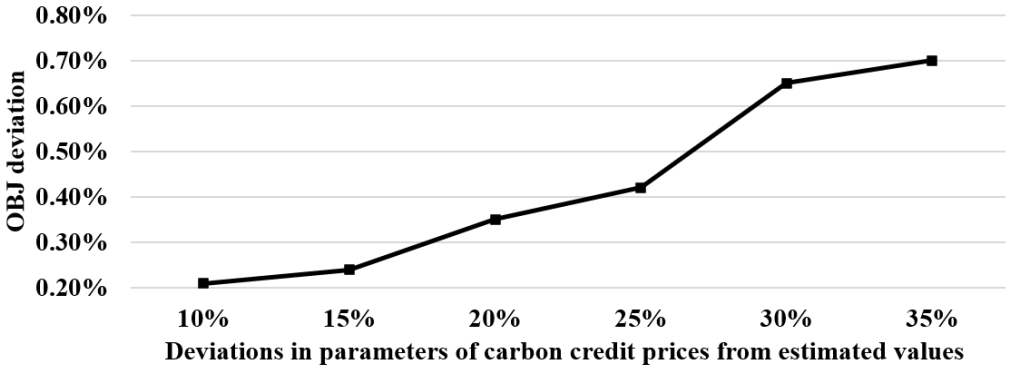

Figure 8: Robustness test of the price of carbon credits

7. Conclusions

This study contributes to the literature in three key respects by integrating blockchain and smart contract technologies into the design of sustainable supply chains.

First, from a modeling perspective, the study introduces a blockchain-enabled two-stage stochastic model to optimize sustainable supply chain operations. The model optimizes facility location and scale decisions under uncertainty and incorporates market-driven carbon management, enabling real-time carbon trading decisions at the operational level. This integration of market mechanisms ensures that carbon credits are dynamically managed, allowing firms to effectively respond to changes in carbon prices and emission levels.

Second, from an algorithm design perspective, the study contributes a method to efficiently solve supply chain problems. Specifically, the proposed primal decomposition algorithm demonstrates high computational efficiency. It effectively solves large-scale and complex supply chain problems within 5 minutes, whereas CPLEX fails to find a solution to these problems even after 1 hour of execution. Moreover, the optimality gap between the results obtained from our algorithm and those achieved by CPLEX is 0%, confirming the algorithm's effectiveness.

Third, from a managerial perspective, the extensive numerical experiments conducted in this study using data from SAIC provide valuable insights for decision-makers. Sensitivity analyses of customer demand, carbon quota ratios, and production capacity levels reveal that, under cap-and-trade regulations, blindly increasing production to meet uncertain demand can lead to higher costs. This finding challenges the conventional notion that increasing production to meet customer demand is always beneficial for

the supply chain. Instead, our study demonstrates that overproduction—without carefully managing carbon credit purchases—can result in unnecessary costs under the carbon trading system. This counter-intuitive result highlights the need for manufacturing companies to strategically plan production capacity while accounting for carbon trading implications to avoid excessive expenses. Moreover, the study emphasizes the importance of strategically allocating carbon credits to minimize total costs. In addition, the stochastic model demonstrates a cost-saving potential of 8.10%, whereas the value of perfect information is 2.32%. The study also indicates that the benefits of blockchain become more pronounced as the scale of the supply chain grows, reducing overall costs. Our robustness tests show that the total cost estimated based on forecasted values deviates by less than 1% from the optimal cost obtained using actual parameters, confirming the model's robustness to fluctuations in carbon credit prices.

Nevertheless, the model has certain limitations. For example, the model assumes a uniform price for carbon credits, whereas distinguishing between the purchase and sale prices would better reflect market dynamics. The impact of supply chain disruptions, such as natural disasters or geopolitical events, is also not considered, which could affect the model's robustness. Future research could explore how disruptions affect the stability and efficiency of supply chains, incorporating risk management strategies and contingency planning into the model. These limitations will guide our future research.

Appendices

Appendix A

Table A provides an overview of the critical input parameters utilized in the mathematical model. Based on the historical sales data of SAIC, the random demand $\tilde{d}_{\omega k}$ from different customers for the product is estimated to follow a uniform distribution $\mathrm{U}(30, 5000)$. For the price of carbon credits related to carbon trading, we base our estimates on data provided by the National Carbon Trading Market Information Network. The total greenhouse gas emissions of SAIC in 2023 were estimated to be 2.03 million metric tons of CO_2 equivalent. The average estimates for e_s^F and e_l^R are 5,000 metric tons each. The fixed costs of the facilities are determined by both the emission control level and the capacity level.

Table A: Key input parameters and setting

Parameters	Setting
Cost of products from location m to n	$g_{mn}^C = 1.5\mathrm{km/RMB} \times l_{mn}$, l_{mn} denotes the distance between location m to n
CO_2 emissions (in kg) of trucks from location m to n	$g_{mn}^E = 1km/kg \times l_{mn}$
Production capacity of producer s with capacity level	$m_{sb}^F = base m_{sb}^F \times TD \times \eta_1, \eta_1 \sim U(0.2, 0.5)$

b; Processing capacity of logistics facility l with capacity level b	$m_{lb}^{R} = basem_{lb}^{R} \times TD \times \eta_2, \eta_2 \sim U(0.2, 0.4)$
Unit production cost of producer s with capacity level b	$k_{sb}^{F} = (1 - 0.05 \times b) \times basek_{sb}^{F}, basek_{sb}^{F} \sim U(50, 3000)$
Unit processing cost of logistics facility l with capacity level b	$n_{lb}^{R} = (1 - 0.01 \times b) \times basen_{lb}^{R}, basen_{lb}^{R} \sim U(10, 30)$
Fixed CO_2 emissions (in kg) with emissions control level c	when c equals 1, 2, 3 respectively, $q_{cs}^{F} = 300, 250, 200 \quad q_{cl}^{R} = 150, 125, 100$
The limited number of carbon credits	$o_s^F = 0.05 \times e_s^F, o_l^R = 0.05 \times e_l^R$
Market price of carbon credits (in RMB)	$c^0 \sim U(65, 120)$
Penalty costs for not meeting customer needs (in RMB)	$c^1 = 5 \times 10^4$

Appendix B

This appendix provides a detailed comparison between our proposed blockchain-integrated model and a model that does not include blockchain technology. In our proposed blockchain-integrated supply chain model, carbon emissions at each node are continuously monitored, and smart contracts automatically trigger carbon credit transactions when emissions exceed a set threshold. In contrast, non–blockchain models lack the ability to make real–time adjustments, as decisions are limited to the initially set carbon quota without the option for carbon credit trading. The comparative model, denoted as $[\mathbf{M3}]$, is outlined below.

$$[\mathbf{M3}] \ \text{Min} \ TC = FC + PL + LC + \sum_{\omega \in \Omega} p_\omega \, \mathcal{Q}(\boldsymbol{\theta}, \omega) \tag{B1}$$

where $FC = \sum_{s \in S} \sum_{c \in C} \sum_{b \in B_s} f_{scb}^{F} \, \alpha_{scb} + \sum_{l \in L} \sum_{c \in C} \sum_{b \in B_l} f_{lcb}^{R} \, \beta_{lcb}$;

$PL = \sum_{s \in S} \sum_{l \in L} \mu_{sl} \left(g_{sl}^{C} + \sum_{c \in C} \sum_{b \in B_s} k_{sb}^{F} \, \alpha_{scb} \right)$;

$LC = \sum_{l \in L} \sum_{k \in K} \theta_{lk} \left(g_{lk}^{C} + \sum_{c \in C} \sum_{b \in B_l} n_{lb}^{R} \beta_{lcb} \right)$.

$$\mathcal{Q}(\boldsymbol{\theta}, \omega) = \left(\widetilde{PL} + \widetilde{LC} \right) + \sum_{\omega \in \Omega} \sum_{l \in L} c^1 \left(\sum_{k \in K} \theta_{lk} - \sum_{k \in K} \tilde{\theta}_{\omega lk} \right)^{+} \tag{B2}$$

where $\widetilde{PL} = \sum_{\omega \in \Omega} \sum_{s \in S} \sum_{l \in L} \tilde{\mu}_{\omega sl} \left(g_{sl}^{C} + \sum_{c \in C} \sum_{b \in B_s} k_{sb}^{F} \, \alpha_{scb} \right)$;

$\widetilde{LC} = \sum_{\omega \in \Omega} \sum_{l \in L} \sum_{k \in K} \tilde{\theta}_{\omega lk} \left(g_{lk}^{C} + \sum_{c \in C} \sum_{b \in B_l} n_{lb}^{R} \, \beta_{lcb} \right)$.

subject to Constraints (2)–(9), (11)–(14)

$$\sum_{c \in C} \sum_{b \in B_s} \alpha_{scb} \, q_{cs}^{F} + \sum_{l \in L} \tilde{\mu}_{\omega sl} g_{sl}^{E} = e_s^F \qquad \forall s \in S, \omega \in \Omega \tag{B3}$$

$$\sum_{c \in C} \sum_{b \in B_l} \beta_{lcb} \, q_{cl}^{R} + \sum_{k \in K} \tilde{\theta}_{\omega lk} g_{lk}^{E} = e_l^R \qquad \forall l \in L, \omega \in \Omega \tag{B4}$$

$$\tilde{\theta}_{\omega lk}, \tilde{\mu}_{\omega sl} \geq 0 \qquad \forall s \in S, l \in L, k \in K, \omega \in \Omega. \tag{B5}$$

The model $[\mathbf{M3}]$ is characterized by the absence of real-time monitoring and automated decision–making mechanisms for carbon trading. Consequently, it lacks the ability to respond instantly to emission fluctuations. The key differences between $[\mathbf{M3}]$ and our proposed model include: The

constraint related to real-time monitoring of carbon emissions using smart contracts, such as $\sum_{c\in C}\sum_{b\in B_s}\alpha_{scb}\,q_{cs}^{F}+\sum_{l\in L}\tilde{\mu}_{\omega sl}g_{sl}^{E}-\tilde{\zeta}_{\omega s}^{+}+\tilde{\zeta}_{\omega s}^{-}\le e_{s}^{F}$ is modified to: $\sum_{c\in C}\sum_{b\in B_s}\alpha_{scb}\,q_{cs}^{F}+\sum_{l\in L}\tilde{\mu}_{\omega sl}g_{sl}^{E}=e_{s}^{F}$. Additionally, decision variables related to carbon trading, such as $\tilde{\zeta}_{\omega s}^{+}$, $\tilde{\zeta}_{\omega s}^{-}$, $\tilde{\eta}_{\omega l}^{+}$ and $\tilde{\eta}_{\omega l}^{-}$ are removed from the constraints and the objective function in the second stage.

References

[1] B. Sundarakani, R. De Souza, M. Goh, S. M. Wagner, and S. Manikandan, "Modeling carbon footprints across the supply chain," Int. J. Prod. Econ., vol. 128, no. 1, pp. 43–50, 2010, doi: 10.1016/j.ijpe.2010.01.018.

[2] P. J. Perez-Martinez, R. M. D. Miranda, and M. D. F. Andrade, "Freight road transport analysis in the metro São Paulo: Logistical activities and CO2 emissions," Transp. Res. Part A: Policy Pract., vol. 137, pp. 16–33, 2020, doi: 10.1016/j.tra.2020.04.015.

[3] M. Yang and X. Chen, "Green technology investment strategies under cap-and-trade policy," IEEE Trans. Eng. Manag., vol. 71, pp. 3867–3880, 2024, doi: 10.1109/TEM.2022.3213947.

[4] X. Xu, P. He, H. Xu, and Q. Zhang, "Supply chain coordination with green technology under cap-and-trade regulation," Int. J. Prod. Econ., vol. 183, pp. 433–442, 2017, doi: 10.1016/j.ijpe.2016.08.029.

[5] T. Zhang, T. M. Choi, and X. Zhu, "Optimal green product's pricing and level of sustainability in supply chains: Effects of information and coordination," Ann. Oper. Res., doi: 10.1007/s10479-018-3084-8, 2018.

[6] L. Soltanisehat, R. Alizadeh, H. Hao, and K. K. R. Choo, "Technical, temporal, and spatial research challenges and opportunities in blockchain-based healthcare: A systematic literature review," IEEE Trans. Eng. Manag., vol. 70, no. 1, pp. 353–368, 2023, doi: 10.1109/TEM.2020.3013507.

[7] Y. Xia, W. Zeng, X. Xing, et al., "Joint optimisation of drone routing and battery wear for sustainable supply chain development: a mixed-integer programming model based on blockchain-enabled fleet sharing," Ann. Oper. Res., vol. 327, pp. 89–127, 2023, doi: 10.1007/s10479-021-04459-5.

[8] Z. Zhang, D. Ren, Y. Lan, and S. Yang, "Price competition and blockchain adoption in retailing markets," Eur. J. Oper. Res., vol. 300, no. 2, pp. 647–660, 2022, doi: 10.1016/j.ejor.2021.08.027.

[9] V. K. Manupati, T. Schoenherr, M. Ramkumar, S. M. Wagner, S. K. Pabba, and R. Raj Singh, "A blockchain-based approach for a multi-echelon sustainable supply chain," Int. J. Prod. Res., vol. 58, no. 7, pp. 2222–2241, 2019, doi: 10.1080/00207543.2019.1683248.

[10] Z. Li, X. Xu, Q. Bai, C. Chen, H. Wang, and P. Xia, "Implications of information sharing on blockchain adoption in reducing carbon emissions: A mean-variance analysis," Transp. Res. Part E: Logist. Transp. Rev., vol. 178, 103254, 2023, doi: 10.1016/j.tre.2023.103254.

[11] A. Döyen, N. Aras, and G. Barbarosoğlu, "A two-echelon stochastic facility location model for humanitarian relief logistics," Optim. Lett., vol. 6, pp. 1123–1145, 2012, doi: 10.1007/s11590-011-0421-0.

[12] L. Cadarso, L. F. Escudero, and A. Marín, "On strategic multistage operational two-stage stochastic 0–1 optimization for the Rapid Transit Network Design problem," Eur. J. Oper. Res., vol. 271, no. 2, pp. 577–593, 2018, doi: 10.1016/j.ejor.2018.05.041.

[13] B. Vahdani, D. Veysmoradi, F. Noori, and F. Mansour, "Two-stage multi-objective location-routing-inventory model for humanitarian logistics network design under uncertainty," Int. J. Disaster Risk Reduc., vol. 27, pp. 290–306, 2018, doi: 10.1016/j.ijdrr.2017.10.015.

[14] N. Kshetri, "Blockchain's roles in meeting key supply chain management objectives," Int. J. Inf. Manag., vol. 39, pp. 80–89, 2018, doi: 10.1016/j.ijinfomgt.2017.12.005.

[15] S. Saberi, M. Kouhizadeh, J. Sarkis, and L. Shen, "Blockchain technology and its relationships to sustainable supply chain management," Int. J. Prod. Res., vol. 57, no. 7, pp. 2117–2135, 2018, doi: 10.1080/00207543.2018.1533261.

[16] M. H. Ali, L. Chung, A. Kumar, S. Zailani, and K. H. Tan, "A sustainable blockchain framework for the halal food supply chain: lessons from Malaysia," Technol. Forecast. Soc. Change, vol. 170, 120870, 2021, doi: 10.1016/j.techfore.2021.120870.

[17] A. A. Mukherjee, R. K. Singh, R. Mishra, and S. Bag, "Application of blockchain technology for sustainability development in agricultural supply chain: Justification framework," Oper. Manag. Res., vol. 15, no. 1, pp. 46–61, 2022, doi: 10.1007/s12063-021-00180-5.

[18] R. Brandín and S. Abrishami, "IoT-BIM and blockchain integration for enhanced data traceability in offsite manufacturing," Automation in Construction, vol. 159, 105266, 2024, doi: 10.1016/j.autcon.2024.105266.

[19] M. K. Lim, H.-Y. Mak, and Z.-J. M. Shen, "Agility and proximity considerations in supply chain design," Manag. Sci., vol. 63, no. 4, pp. 1026–1041, 2016, doi: 10.1287/mnsc.2015.2380.

[20] K. Govindan, M. Fattahi, and E. Keyvanshokooh, "Supply chain network design under uncertainty: a

comprehensive review and future research directions," Eur. J. Oper. Res., vol. 263, no. 1, pp. 108–141, 2017, doi: 10.1016/j.ejor.2017.04.009.
[21] K. Govindan, H. Soleimani, and D. Kannan, "Reverse logistics and closed-loop supply chain: a comprehensive review to explore the future," Eur. J. Oper. Res., vol. 240, no. 3, pp. 603–626, 2015, doi: 10.1016/j.ejor.2014.07.012.
[22] S. A. R. Khan, D. I. Godil, C. J. C. Jabbour, S. Shujaat, A. Razzaq, and Z. Yu, "Green data analytics, blockchain technology for sustainable development, and sustainable supply chain practices: evidence from small and medium enterprises," Ann. Oper. Res., 2021, doi: 10.1007/s10479-021-04275-x.
[23] F. Wang, X. Lai, and N. Shi, "A multi-objective optimization for green supply chain network design," Decis. Support Syst., vol. 51, no. 2, pp. 262–269, 2011, doi: 10.1016/j.dss.2010.11.020.
[24] Z. Z. Zhong and E. Y. Zhao, "Collaborative driving mode of sustainable marketing and supply chain management supported by Metaverse technology," IEEE Trans. Eng. Manag., vol. 71, pp. 1642–1654, 2024, doi: 10.1109/TEM.2023.3337346.
[25] C. Waltho, S. Elhedhli, and F. Gzara, "Green supply chain network design: a review focused on policy adoption and emission quantification," Int. J. Prod. Econ., vol. 208, pp. 305–318, 2019, doi: 10.1016/j.ijpe.2018.12.003.
[26] L. Chen, Y. Wang, J. Peng, and Q. Xiao, "Supply chain management based on uncertainty theory: a bibliometric analysis and future prospects," Fuzzy Optim. Decis. Making, vol. 23, pp. 599–636, 2024, doi: 10.1007/s10700-024-09435-9.
[27] M. S. Pishvaee, S. A. Torabi, and J. Razmi, "Credibility-based fuzzy mathematical programming model for green logistics design under uncertainty," Comput. Ind. Eng., vol. 62, no. 2, pp. 624–632, 2012, doi: 10.1016/j.cie.2011.11.028.
[28] L. Zhen, L. Huang, and W. Wang, "Green and sustainable closed-loop supply chain network design under uncertainty," J. Clean. Prod., vol. 227, pp. 1195–1209, 2019, doi: 10.1016/j.jclepro.2019.04.098.
[29] H. Kaur, S. P. Singh, J. A. Garza-Reyes, and N. Mishra, "Sustainable stochastic production and procurement problem for resilient supply chain," Comput. Ind. Eng., vol. 139, p. 105560, 2020, doi: 10.1016/j.cie.2018.12.007.
[30] A. Hasani, H. Mokhtari, and M. Fattahi, "A multi-objective optimization approach for green and resilient supply chain network design: a real-life case study," J. Clean. Prod., vol. 278, p. 123199, 2021, doi: 10.1016/j.jclepro.2020.123199.
[31] Kumar and K. Kumar, "An uncertain sustainable supply chain network design for regulating greenhouse gas emission and supply chain cost," Clean. Logist. Supply Chain., vol. 10, Art. no. 100142, 2024, doi: 10.1016/j.clscn.2024.100142.
[32] L. Dong, P. (P.) Jiang, and F. Xu, "Impact of traceability technology adoption in food supply chain networks," Manage. Sci., vol. 69, no. 3, pp. 1518-1535, 2022, doi: 10.1287/mnsc.2022.4440.
[33] P. Singh, Z. Elmi, Y.-y. Lau, M. Borowska-Stefańska, S. Wiśniewski, and M. A. Dulebenets, "Blockchain and AI technology convergence: applications in transportation systems," Veh. Commun., vol. 38, Art. no. 100521, 2022, doi: 10.1016/j.vehcom.2022.100521.
[34] S. S. Kamble, A. Gunasekaran, N. Subramanian, A. Ghadge, A. Belhadi, and M. Venkatesh, "Blockchain technology's impact on supply chain integration and sustainable supply chain performance: evidence from the automotive industry," Ann. Oper. Res., vol. 327, no. 1, pp. 575-600, 2023, doi: 10.1007/s10479-021-04129-6.
[35] F. Zhang and W. Song, "Sustainability risk assessment of blockchain adoption in sustainable supply chain: An integrated method," Comput. Ind. Eng., vol. 171, 108378, 2022, doi: 10.1016/j.cie.2022.108378.
[36] J. Zhu, T. Feng, Y. Lu, and W. Jiang, "Using blockchain or not? a focal firm's blockchain strategy in the context of carbon emission reduction technology innovation," Bus. Strategy Environ., vol. 33, no. 4, pp. 3505–3531, 2024, doi: 10.1002/bse.3664.
[37] Q. Li, X. Guan, T. Shi, and W. Jiao, "Green product design with competition and fairness concerns in the circular economy era," Int. J. Prod. Res., vol. 58, no. 1, pp. 165–179, 2019, doi: 10.1080/00207543.2019.1657249.
[38] R. K. Singh, K. Mathiyazhagan, V. Scuotto, and M. Pironti, "Green open innovation and circular economy: investigating the role of big data management and sustainable supply chain," IEEE Trans. Eng. Manag., vol. 71, pp. 8417–8429, 2024, doi: 10.1109/TEM.2024.3387107.
[39] T. Zhang, P. Li, and N. Wang, "Multi-period price competition of blockchain-technology-supported and traditional platforms under network effect," Int. J. Prod. Res., vol. 61, no. 11, pp. 3829–3843, 2021, doi: 10.1080/00207543.2021.1884308.
[40] Q. Li, M. Ma, T. Shi, and C. Zhu, "Green investment in a sustainable supply chain: the role of blockchain and fairness," Transp. Res. Part E: Logist. Transp. Rev., vol. 167, Art. no. 102908, 2022, doi: 10.1016/j.tre.2022.102908.
[41] T. M. Choi and S. Luo, "Data quality challenges for sustainable fashion supply chain operations in emerging

markets: roles of blockchain, government sponsors, and environment taxes," Transp. Res. Part E: Logist. Transp. Rev., vol. 131, pp. 139–152, 2019, doi: 10.1016/j.tre.2019.09.019.
[42] S. Guo, X. Sun, and H. K. S. Lam, "Applications of blockchain technology in sustainable fashion supply chains: operational transparency and environmental efforts," IEEE Trans. Eng. Manag., vol. 70, no. 4, pp. 1312–1328, 2023, doi: 10.1109/TEM.2020.3034216.
[43] Z. El Hathat, V. G. Venkatesh, T. Zouadi, V. R. Sreedharan, A. Manimuthu, and Y. Shi, "Analyzing the greenhouse gas emissions in the palm oil supply chain in the VUCA world: a blockchain initiative," Bus. Strategy Environ., vol. 32, no. 8, pp. 5563–5582, 2023, doi: 10.1002/bse.3436.
[44] X. Xu, L. Yan, T. M. Choi, and T. C. E. Cheng, "When is it wise to use blockchain for platform operations with remanufacturing?" Eur. J. Oper. Res., vol. 309, no. 3, pp. 1073–1090, 2023, doi: 10.1016/j.ejor.2023.01.063.
[45] S. Yousefi and B. M. Tosarkani, "Exploring the role of blockchain technology in improving sustainable supply chain performance: a system-analysis-based approach," IEEE Trans. Eng. Manag., vol. 71, pp. 4389–4405, 2024, doi: 10.1109/TEM.2022.3231217.
[46] A. Corallo, M. E. Latino, M. Menegoli, and F. Signore, "Digital technologies for sustainable development of agri-food: implementation guidelines toward industry 5.0," IEEE Trans. Eng. Manag., vol. 71, pp. 10699–10715, 2024, doi: 10.1109/TEM.2024.3403251.
[47] K. Nayal, R. D. Raut, B. E. Narkhede, P. Priyadarshinee, G. B. Panchal, and V. V. Gedam, "Antecedents for blockchain technology-enabled sustainable agriculture supply chain," Ann. Oper. Res., vol. 327, no. 1, pp. 293–337, 2023, doi: 10.1007/s10479-021-04423-3.
[48] H. Hasan, E. AlHadhrami, A. AlDhaheri, K. Salah, and R. Jayaraman, "Smart contract-based approach for efficient shipment management," Comput. Ind. Eng., vol. 136, pp. 149–159, 2019, doi: 10.1016/j.cie.2019.07.022.
[49] Y. Li, M. K. Lim, and C. Wang, "An intelligent model of green urban distribution in the blockchain environment," Resour. Conserv. Recycl., vol. 176, Art. no. 105925, 2022, doi: 10.1016/j.resconrec.2021.105925.
[50] W. Li, L. Wang, Y. Li, and B. Liu, "A blockchain-based emissions trading system for the road transport sector: Policy design and evaluation," Clim. Policy, vol. 21, no. 3, pp. 337–352, 2020, doi: 10.1080/14693062.2020.1851641.
[51] T. K. Agrawal, V. Kumar, R. Pal, L. Wang, and Y. Chen, "Blockchain-based framework for supply chain traceability: A case example of textile and clothing industry," Comput. Ind. Eng., vol. 154, Art. no. 107130, 2021, doi: 10.1016/j.cie.2021.107130.
[52] A. A. Sadawi, B. Madani, S. Saboor, M. Ndiaye, and G. Abu-Lebdeh, "A comprehensive hierarchical blockchain system for carbon emission trading utilizing blockchain of things and smart contract," Technol. Forecast. Soc. Change, vol. 173, Art. no. 121124, 2021, doi: 10.1016/j.techfore.2021.121124.
[53] S. Ismail, M. Nouman, H. Reza, F. Vasefi, and H. K. Zadeh, "A blockchain-based fish supply chain framework for maintaining fish quality and authenticity," IEEE Trans. Services Comput., vol. 17, no. 5, pp. 1877–1886, 2024, doi: 10.1109/TSC.2024.3422897.
[54] D. Prajapati, S. K. Jauhar, A. Gunasekaran, S. S. Kamble, and S. Pratap, "Blockchain and IoT embedded sustainable virtual closed-loop supply chain in e-commerce towards the circular economy," Comput. Ind. Eng., vol. 172, Part A, Art. no. 108530, 2022, doi: 10.1016/j.cie.2022.108530.

Jingwen Wu is a Ph.D. student at School of Management, Shanghai University, Shanghai, China. Her research interests include operations management and optimization; mixed-integer linear programming and algorithms; maritime shipping optimization; urban logistics and supply chain management. She has published 11 papers on SCI international journals such as IISE Transactions, Transportation Research Part E, Journal of the Operational Research Society, Computers & Operations Research, Annals of Operations Research.

Yuting Yan is a Master student at School of Management, Shanghai University, Shanghai, China. Her research interests include optimization problems on blockchain and supply chain management.

Shuaian Wang is a Professor at Faculty of Business, The Hong Kong Polytechnic University, Hong Kong, China. His research interests include big data in shipping, green shipping, shipping operations management, port planning and operations, urban transport network modeling, and logistics and supply chain management. He is an editor-in-chief of Cleaner Logistics and Supply Chain and Communications in Transportation Research, a co-editor-in-chief of Transportation Research Part E, an associate editor of Flexible Services and Manufacturing Journal, Transportmetrica A, and Transportation Letters, a handle editor of Transportation Research Record, an editorial board editor of Transportation Research Part B, and an editorial board member of Maritime Transport Research.

Lu Zhen is a Professor and Dean at School of Management, Shanghai University, Shanghai, China. His research interests include operations management and optimization; mixed-integer linear programming and algorithms; port operations and maritime transportation; urban logistics and supply chain management. He has served as an associate editor or an editorial board member of five journals such as Transportation Research Part B, Journal of the Operational Research Society, Computers & Operations Research; and he is also the Fellow of the Operational Research Society (U.K.). He has been awarded the National Funds for Distinguished Young Scientists, for Outstanding Young Scientists in China, the Changjiang Young Scholar in China, and etc.